

Environmental setting of deep-water oysters in the Bay of Biscay

D. Van Rooij^{a,*}, L. De Mol^a, E. Le Guilloux^b, M. Wisshak^c, V.A.I. Huvenne^d, R. Moeremans^{e,a},
J.-P. Henriët^a

^a Renard Centre of Marine Geology, Ghent University, Krijgslaan 281 S8, B-9000 Gent, Belgium

^b IFREMER, Laboratoire Environnement Profond, BP70, F-29280 Plouzané, France

^c GeoZentrum Nordbayern, Erlangen University, Loewenichstr. 28, D-91054 Erlangen, Germany

^d Geology and Geophysics Group, National Oceanography Centre, European Way, SO14 3 ZH Southampton, UK

^e Scripps Institution of Oceanography, UCSD, La Jolla, CA, United States of America

*: Corresponding author : David Van Rooij, Tel.: +32 9 2644583 ; fax: +32 9 2644967 ;

email address : david.vanrooij@ugent.be

Abstract :

We report the northernmost and deepest known occurrence of deep-water pycnodontine oysters, based on two surveys along the French Atlantic continental margin to the La Chapelle continental slope (2006) and the Guilvinec Canyon (2008). The combined use of multibeam bathymetry, seismic profiling, CTD casts and a remotely operated vehicle (ROV) made it possible to describe the physical habitat and to assess the oceanographic control for the recently described species *Neopycnodonte zibrowii*. These oysters have been observed in vivo in depths from 540 to 846 m, colonizing overhanging banks or escarpments protruding from steep canyon flanks. Especially in the Bay of Biscay, such physical habitats may only be observed within canyons, where they are created by both long-term turbiditic and contouritic processes. Frequent observations of sand ripples on the seabed indicate the presence of a steady, but enhanced bottom current of about 40 cm/s. The occurrence of oysters also coincides with the interface between the Eastern North Atlantic Water and the Mediterranean Outflow Water. A combination of this water mass mixing, internal tide generation and a strong primary surface productivity may generate an enhanced nutrient flux, which is funnelled through the canyon. When the ideal environmental conditions are met, up to 100 individuals per m² may be observed. These deep-water oysters require a vertical habitat, which is often incompatible with the requirements of other sessile organisms, and are only sparsely distributed along the continental margins. The discovery of these giant oyster banks illustrates the rich biodiversity of deep-sea canyons and their underestimation as true ecosystem hotspots.

Research Highlights

► *Neopycnodonte zibrowii* oysters occur in a bathymetric range between 350 and 846 m. ► *N. zibrowii* habitat requires steep slopes with overhanging banks and escarpments. ► This underestimated deep-water community occurs almost exclusively in canyons. ► Suitable habitats created by interplay between turbiditic and contouritic processes.

Keywords : Bay of Biscay ; Deep-water oysters ; Canyons ; Habitat ; Resuspension ; MOW ; *Neopycnodonte zibrowii*

1 52 **1. Introduction**

2
3 53 Ocean margins are dynamic environments which host valuable deep-water benthic
4
5
6 54 ecosystems. Along the Eastern Atlantic margin from Morocco to Norway, several
7
8 55 „deep-water ecosystem hotspots’ have been identified in association with a complex
9
10 56 interplay of oceanography, geology, seabed morphology, sediment and nutrient supply
11
12
13 57 (Weaver and Gunn, 2009). Cold-water coral reefs and canyon environments are
14
15
16 58 receiving particularly close attention (Arzola et al., 2008; Canals et al., 2006; De Mol et
17
18 59 al., accepted; de Stigter et al., 2007; Dorschel et al., 2009; Mienis et al., 2007;
19
20 60 Palanques et al., 2009; Wienberg et al., 2009). Cold-water coral occurrences have been
21
22
23 61 identified over virtually the entire European margin and their reefs feature a high
24
25 62 biodiversity (Freiwald et al., 2004; Reveillaud et al., 2008; Roberts et al., 2006). They
26
27
28 63 belong to the Earth's most precious and endangered ecosystems, threatened by fisheries
29
30 64 and ocean acidification (Freiwald et al., 2004; Halpern et al., 2008; IPCC, 2007; Roberts
31
32 65 et al., 2006). The main driver for this ecosystem is a carefully balanced hydrodynamic
33
34
35 66 environment controlling sediment and nutrient supply (Dorschel et al., 2009; Mienis et
36
37 67 al., 2007; Roberts et al., 2006). Canyons play a critical role since they are the most
38
39
40 68 important mechanism of nutrient input into the deep marine environment (Canals et al.,
41
42 69 2006; de Stigter et al., 2007; Duineveld et al., 2001; Palanques et al., 2009). Moreover,
43
44 70 due to frequent incisions during glacial sea-level lowstands (Bourillet et al., 2006;
45
46 71 Cunningham et al., 2005; Toucanne et al., 2009; Zaragosi et al., 2000), the eroded
47
48 72 canyon flanks may offer a peculiar environment which is beneficial for settling of
49
50 73 sessile organisms since they profit from the enhanced nutrient flux. Already in the late
51
52 74 19th and the mid-20th century fisheries research had demonstrated the presence of cold-
53
54
55 75 water corals in the vicinity of the canyons in the northern Bay of Biscay (Reveillaud et
56
57
58
59
60
61
62
63
64
65

1 76 al., 2008). A first mapping and description of these *Massifs coralliens* (Fig. 1) was
2
3 77 published by Le Danois (1948). Sporadically, scientists and fishermen also reported
4
5 78 dredged oysters from this part of the margin, which was not given the appropriate
6
7
8 79 attention at that time. Oysters are commonly referred to as typical shallow-water and
9
10
11 80 occasionally reef-forming molluscs, but a number of samples have also been recovered
12
13 81 from the deeper realm (Wisshak et al., 2009a). The existence of the deep-water oyster
14
15 82 *Neopycnodonte zibrowii* was formally described in Wisshak et al. (2009a) based on
16
17
18 83 submersible observations and sampling in the Azores archipelago between 2002 and
19
20 84 2007.

21
22
23 85
24
25 86 In this paper, we report and describe the physical and oceanographic setting of the
26
27 87 northernmost and deepest occurrence of *Neopycnodonte zibrowii* oysters within two
28
29 88 canyons along the French Atlantic margin (Fig. 1). Seabed observations with the
30
31 89 Remotely Operated Vehicle (ROV) *Genesis* resulted in the discovery of giant deep-
32
33 90 water oyster banks and cliffs in depths between 540 to 846 m (Table 1). These
34
35
36
37 91 observations were performed with R/V *Belgica* during the HERMES Geo cruise in June
38
39 92 2006 (La Chapelle continental slope) and the BiSCOSYSTEMS cruise in June 2008
40
41 93 (Guilvinec canyon). The observed spatial distribution of the molluscs in relation to the
42
43 94 slope morphology and local hydrographic regime gives an insight in the habitat
44
45 95 requirements of this new species. This will be compared to the habitat requirements of
46
47
48 96 another successful reef-forming organism: scleractinian cold-water corals.
49
50

51 97

52 98 **2. Regional setting**

53
54
55
56
57
58
59
60
61
62
63
64
65

1 99 The NE Atlantic continental margin in the Bay of Biscay can be divided in five main
2
3 100 areas: the Celtic and the Armorican margin in the north, and the Aquitaine, Cantabrian
4
5 101 and Galician margin in the south (Fig. 1). The morphology of the continental slope is
6
7 102 characterized by spurs and canyons, organized in drainage basins and actively feeding
8
9 103 the Celtic, Armorican and Cap Ferret deep-sea fans (Bourillet et al., 2003; Zaragosi et
10
11 104 al., 2000). However, between the Delesse (47°N) and Conti Spur (45°N), no significant
12
13 105 deep-sea fans are observed at the mouth of the lower (southern) valleys; only small
14
15 106 channel-levee complexes, slumps and small lobes are present (Bourillet et al., 2006).
16
17 107
18
19 108 Most of the water masses in the Bay of Biscay are of North Atlantic origin (Pollard *et*
20
21 109 *al.*, 1996). The uppermost water mass is the Eastern North Atlantic (Central) Water
22
23 110 (ENAW), which extends to depths of about 400 to 600 m. Although this water mass has
24
25 111 a salinity of 35.6, according to Pollard et al. (1996) there is a core of low density water
26
27 112 around 500 m water depth due to the lateral influence of the Subarctic Intermediate
28
29 113 Water (SAIW). Between 400 to 500 m and 1500 m water depth, the Mediterranean
30
31 114 Outflow Water (MOW) follows the continental slope as a contour current. Its
32
33 115 circulation is conditioned by seafloor irregularities and the Coriolis effect. MOW
34
35 116 velocities have been measured in the Bay of Biscay at 8°W and 6°W with minimum
36
37 117 values of 2-3 cm/s. Iorga and Lozier (1999) show that the MOW splits into two
38
39 118 branches as it passes Galicia Bank, and turns into the Bay of Biscay as a cyclonic
40
41 119 recirculation. Low salinity values observed on the Armorican continental slope may
42
43 120 reflect a depletion of the MOW core (Van Aken, 2000). Between 1500 and 3000 m
44
45 121 water depth the North Atlantic Deep Water (NADW) is recognized. It includes a core of
46
47 122 the Labrador Sea Water (LSW) at a depth of about 1800 m down to 2000 m
48
49
50
51
52
53
54
55
56
57
58
59
60
61
62
63
64
65

1 123 (McCartney, 1992; McCave et al., 2001; Vangriesheim and Khripounoff, 1990). Below
2
3 124 the NADW, the Lower Deep Water is identified, which mainly seems to result from the
4
5 125 mixing of the deep Antarctic Bottom Water and the Labrador Deep Water (Botas et al.,
6
7
8 126 1989; Haynes and Barton, 1990; Pingree and Le Cann, 1992; Van Aken, 2000).
9

10 127
11
12 128 Along the slopes of the Bay of Biscay strong, localized internal tides are reported,
13
14 129 resulting from a combination of favourable water mass stratification, steep topography
15
16 130 and strong barotropic tidal currents (Huthnance, 1995; Pairaud et al., 2008; Pingree and
17
18 131 Le Cann, 1989, 1990). As the slope is intersected with canyons, these tidally induced
19
20 132 transports may be channelled and result in regions of locally increased flow and local
21
22 133 circulations (Pingree and Le Cann, 1990). A dominant effect caused by internal tides
23
24 134 from the upper slope is proposed to explain the enhanced levels of surface
25
26 135 phytoplankton abundance (Holligan et al., 1985; Pingree et al., 1982).
27
28
29
30
31
32

33 136

35 137 **3. Material and methods**

36
37 138 The data for this study was acquired during two R/V Belgica expeditions in the Bay of
38
39 139 Biscay. A first cruise, HERMES Geo, focussed during only 3 days in June 2006 on the
40
41 140 La Chapelle continental slope (Fig. 1b). In June 2008, the BiSCOSYSTEMS cruise
42
43 141 surveyed the vicinity of the Guilvinec Canyon (Fig. 1c). During both cruises a
44
45 142 geophysical survey (multibeam bathymetry and seismic profiling) and CTD profiling
46
47 143 (Fig. 2) preceded the ROV observations.
48
49
50

51 144

54 145 **3.1 Geophysical survey**

56
57
58
59
60
61
62
63
64
65

1 146 Initial swath bathymetry coverage of both study areas was performed using the R/V
2
3 147 Belgica hull-mounted SIMRAD EM1002 multibeam echosounder. On the La Chapelle
4
5 148 continental slope, an area of 71.7 km² was mapped in water depths ranging from 200 to
6
7
8 149 950 m (Fig. 1b) and processed using the IFREMER CARAIBES software. In 2008, an
9
10 150 area of 584 km² was mapped around the Guilvinec canyon in water depths ranging from
11
12
13 151 180 to 1000 m (Fig. 1c). The 2008 dataset was processed using MB-Systems and IVS
14
15 152 Fledermaus software. Both datasets were gridded to a cell size of 20 by 20 m and
16
17
18 153 visualized using GMT version 4.2 (Wessel and Smith, 1991).

19
20 154
21
22 155 In order to obtain insight in the sedimentary processes and the thickness of the sediment
23
24
25 156 cover, single channel seismic profiles were acquired using a SIG sparker source at a
26
27
28 157 velocity of 3 knots (Figs. 1c and 3). The source was triggered every 3 s, reaching 500 J
29
30 158 energy. The vertical resolution of the profiles varies between 1 and 2 m. A basic
31
32
33 159 processing (band-pass filtering, automatic gain control) was applied using PROMAX
34
35 160 software.

36
37 161

40 162 ***3.2 Water mass characterization***

41
42 163 At both sites, information regarding the water mass stratification was obtained using a
43
44
45 164 SEACAT SBE 19 CTD down to water depths of about 1400 m (Table 2, Fig. 2). The
46
47
48 165 raw data was binned at 1 m using SBE Data Processing (version 7.16a). The obtained
49
50 166 temperature (°C), salinity and potential density (sigma-theta, kg/m³) were used to
51
52 167 identify the water masses and to indicate the relationship between deep-water oyster
53
54
55 168 occurrence and hydrography (Fig. 2).

56
57 169

58
59
60
61
62
63
64
65

1 170 **3.3 ROV observations**
2
3 171 The ROV observations (Table 1, video files as online supplementary material) were
4
5
6 172 performed using Ghent University's ROV *Genesis*, a Sub Atlantic Cherokee type ROV
7
8 173 with a Tethered Management System (TMS) allowing investigations down to 1400 m
9
10 174 water depth. The underwater positioning was obtained using an IXSEA GAPS USBL
11
12 175 system, allowing an accuracy in the order of 2 m. Seafloor observations were made by
13
14 176 means of a forward-looking colour zoom and black & white video camera, assisted by >
15
16 177 250 Watt Q-LED illumination. A laser marker was added to the camera head for scale
17
18 178 (10 cm spacing). High-resolution images were acquired using a digital Canon
19
20 179 Powershot stills camera. Unfortunately, due to a malfunctioning during the June 2006
21
22 180 campaign, images were derived from video capture instead of the stills camera. The
23
24 181 processing and interpretation of dive B06-02 was performed in an ArcGIS environment,
25
26 182 expanded with the Adélie extension for ArcGIS 9.0 developed at IFREMER
27
28 183 (http://www.ifremer.fr/flotte/systemes_sm/adelie/index.html). Dives B08-02 and B08-
29
30 184 05 were interpreted using OFOP (Ocean Floor Observation Protocol) version 3.2.0c
31
32 185 (Huetten and Greinert, 2008) and integrated into ArcGIS.
33
34
35
36
37
38
39
40
41

42 187 **4. Results**

43 188 **4.1 Environmental setting**

44 189 **4.1.1 Hydrography**

45 190 The CTD casts show a similar water mass stratification in both study areas (Fig. 2). The
46
47 191 seasonal thermocline is recognized down to 50 m water depth (Figs. 2b-c). A salinity
48
49 192 minimum (± 35.58) at about 550 m separates the upper Eastern North Atlantic Water
50
51 193 (ENAW) from the saline Mediterranean Outflow Water (MOW), which has its salinity
52
53
54
55
56
57
58
59
60
61
62
63
64
65

1 194 maximum (± 35.76) at about 1000 m. Below, the T/S profile gradually follows the 27.75
2
3 195 kg/m^3 potential density gradient towards the LSW and NADW.
4

5
6 196

7
8 197 *4.1.2 Geomorphology*
9

10 198 The morphology of the La Chapelle continental slope is characterized by spurs and
11
12 199 canyons (Fig. 1b). This study was carried out around a central, yet unnamed spur,
13
14 200 flanked by deep canyons and thalweg channels in surveyed water depths from 150 to
15
16 201 1100 m. It has a main NE-SW orientation and an average inclination of 2° . Based on
17
18 202 our discoveries, we suggest the name *Ostrea Spur* for this morphological feature. The
19
20 203 slopes flanking the spur show a ‚herringbone‘ pattern of WNW-ESE orientated gullies
21
22 204 on the western slope ($13\text{-}15^\circ$) and NNW-SSE orientated gullies on the eastern slope
23
24 205 (16°).
25
26
27
28
29

30 206

31
32 207 The Armorican margin near the Guilvinec Canyon is characterised by a heavily incised
33
34 208 slope with NE-SW oriented canyons and spurs (Fig. 1). The Guilvinec Canyon is 14 km
35
36 209 wide and bound to the northwest by the Penmarc’h Spur. The main part of this spur is
37
38 210 relatively flat ($0\text{-}2^\circ$) until 250 m water depth. Here, the gradient towards the Guilvinec
39
40 211 Canyon is rather abrupt (10°), especially along its relatively steep northern to north-
41
42 212 western flanks ($30\text{-}40^\circ$). This flank contains about 4 large dendritic gully systems with a
43
44 213 NNW-SSE orientation. In contrast, the eastern flank of the canyon is much smoother
45
46 214 (and less incised) with slope gradients ranging from 5 to maximum 20° . This
47
48 215 asymmetry is also observed on the seismic profiles (Figs. 1c and 3). Figure 3b shows a
49
50 216 seismic profile through the largest (1 km wide) and steepest ($17\text{-}35^\circ$) gully, which was
51
52
53
54
55 217 also the subject of ROV dive B08-02 (Fig. 1c). Exclusively on the SE flank, a large
56
57
58
59
60
61
62
63
64
65

1 218 (200-400 ms TWT) sigmoidal depositional sequence can be observed which explains
2
3 219 the smoother slope texture. A comparison with other regional seismic stratigraphic
4
5 220 studies (Bourillet et al., 2003; Paquet et al., 2010) suggests that this sequence may be
6
7 221 correlated with the Pliocene to Pleistocene Little Sole Formation. On the other hand,
8
9 222 almost the entire NW flank is covered with diffraction hyperbolae, suggesting erosive
10
11 223 steep slopes, irregular topography or outcropping hard substratum. These deeper strata
12
13 224 may have a Miocene origin, belonging to the Jones or Cockburn Formations (Bourillet
14
15 225 et al., 2003). Along the south-western tip of the spur, 6 more gullies can be observed
16
17 226 within the prolongation of the spur's axis. These gullies are approximately 400-500 m
18
19 227 wide and have a gradient between 10 to 25°.
20
21
22
23
24

25 228

27 229 ***4.2 ROV observations***

30 230 *4.2.1 Dive B06-02: Eastern flank of Ostrea Spur*

31 231 Dive B06-02 followed a SW-NW, 2800 m long track over the eastern flank of the
32
33 232 Ostrea Spur, parallel to its elongation, crossing several of the steep (16°) NNW-SSE
34
35 233 orientated gullies on the eastern slope (Fig. 4). The main observations were carried out
36
37 234 on the central gully between 7°20'00"W and 7°19'40"W, allowing a more
38
39 235 comprehensive view on the gully environment.
40
41
42
43
44

45 236

46
47 237 A large part of the dive trajectory (57%) showed sandy bioturbated sediments with
48
49 238 ripple marks on the relatively flat gully shoulders (Figs. 4 and 5a). These fairly straight
50
51 239 NW-SE oriented sand ripples have wavelengths of approximately 10-20 cm and are less
52
53 240 than 10 cm high. On other locations outside the gully axis, an enigmatic pale-coloured
54
55 241 facies was observed featuring decimetric to metric blocks or knolls inferred to be
56
57
58
59
60
61
62
63
64
65

1 242 carbonated material (Fig. 5b). No recent sediment cover was observed and frequently
2
3 243 yellow *Hexadella* sp. sponges were noticed on top these blocks, which were observed
4
5
6 244 over 25% of the track length.
7
8 245
9
10 246 Protruding banks with a thickness ranging from 10 to 30 cm were observed regularly,
11
12 247 especially on the steep slopes within the central part of the dive between 620 and 680 m
13
14 248 (Figs. 5c-d). They form steps down to the central gully thalweg along a NNE-SSW to
15
16 249 NW-SE orientation (Fig. 4). In total, 20 laterally variable banks were encountered over
17
18 250 60 m depth. Towards the centre of the gully they disappear into a large N-S oriented
19
20 251 escarpment between 630 and 650 m water depth (Fig. 5f). Based on our observations,
21
22 252 this escarpment cliff is at least 10 m high. The ensemble of this steep environment
23
24 253 represents about 16% of the track length. At the base of this cliff and above the larger
25
26 254 banks, accumulated debris provides settling sites for sessile organisms, whilst the
27
28 255 escarpment and the larger protruding banks are sporadically colonized by medium to
29
30 256 dense communities of giant (10-15 cm) *Neopycnodonte zibrowii* oysters (Figs. 5d-e),
31
32 257 forming a 3D assemblage with occasional dead cold-water corals (*Lophelia pertusa*),
33
34 258 which occur very rarely. The oysters only occur in high densities (up to 100 individuals
35
36 259 per m²) near the centre of the gully between 620 and 680 m, while they were also
37
38 260 observed in a similar setting at 4 other locations between 540 to 680 m (Fig. 4). Most
39
40 261 typically, at the side of the gully, they only occur underneath overhanging banks which
41
42 262 protrude far enough (10-15 cm) from the seafloor. Only 9 of the observed banks were
43
44 263 large enough to offer sufficient space for closely stacked shells, literally hanging in a
45
46 264 density of about 30 individuals per m² (Fig. 5e). Near the escarpment, they act as a high-
47
48 265 density vertical wall pavement (Fig. 5f). Many oyster individuals are still articulated and
49
50
51
52
53
54
55
56
57
58
59
60
61
62
63
64
65

1 266 alive, or, where the free right valve is detached, show the non-degraded and locally still
2
3 267 dark-coloured endostracum indicating that these oysters died only recently (Fig. 5e).
4
5
6 268
7
8 269 *4.2.2 Dive B08-02: North-western flank of Guilvinec Canyon*
9
10 270 Dive B08-02 covered 3700 m of seafloor observations along a U-shaped track starting
11
12 271 with the first “leg” southwards from the NE flank of a gully at 700 m water depth and
13
14 272 ending with a second “leg” parallel to the gully axis (Figs. 1c and 6). The seabed slope
15
16 273 along this track has an average gradient of 11°.
17
18
19
20 274
21
22 275 Along the main part of the dive track, a featureless bioturbated sandy seafloor was
23
24 276 observed. Nevertheless, the easternmost part of the track which is roughly following
25
26 277 5°22’50”W, revealed the presence of abundant yellow *Hexadella* sp. sponges, live
27
28 278 *Madrepora oculata* patches or fossil *Lophelia pertusa* debris (Fig. 6). Since the
29
30 279 distribution, diversity and habitat settings of cold-water corals along this part of the
31
32 280 Armorican margin are discussed in detail by De Mol et al. (accepted), only their
33
34 281 occurrence and substratum are described in this section. These are predominantly
35
36 282 solitary cold-water corals and represent about 40% of the observations. The present-day
37
38 283 community is not forming close reef-like structures, but can be found on dead cold-
39
40 284 water coral rubble “graveyards” (De Mol et al., accepted). Further observed substrates
41
42 285 for the cold-water corals include a sandy rippled seabed, buried biogenic rubble and
43
44 286 erratic boulders. Common, co-occurring organisms associated to the cold-water corals
45
46 287 are sea-pens, sea-urchins, sponges and soft corals (De Mol et al., accepted).
47
48
49
50 288
51
52
53
54
55
56
57
58
59
60
61
62
63
64
65

1 289 Between 800 and 950 m, a rippled seabed was frequently encountered (10% of the
2
3 290 observations). Especially below 900 m, straight and sometimes sinuous N-S oriented
4
5 291 low-relief sand ripples were observed with wavelengths ranging between 10-20 cm and
6
7
8 292 heights of approximately 5 cm (Figs. 6 and 7c). Additionally, relatively intense
9
10 293 flocculation was noted (Fig. 7c).

11
12 294
13
14
15 295 Only sporadically (less than 5% of the observations), the rather smoothly sloping seabed
16
17 296 is interrupted by small banks or escarpments (Figs. 6 and 7a-b). These escarpments are
18
19 297 long “ruptures” in the seabed, showing a consolidated substrate and having an E-W
20
21 298 orientation between 700 and 750 m, while the ones located deeper than 750 m, usually
22
23 299 show a S-N or SSW-NNE orientation. Generally, the banks have a decimetric scale,
24
25 300 while the heights of the escarpments range between 2 to 4 m. On only at three out of
26
27 301 nine locations (Figs. 6 and 7a-c), the escarpments were colonized by *Neopycnodonte*
28
29 302 *zibrowii* oysters and, in lesser degree, by *Madrepora oculata*. However, compared to
30
31 303 dive B06-02 on Ostrea Spur, the abundance of *Neopycnodonte zibrowii* on the
32
33 304 escarpments (Figs. 7a-b), is far less with 10 to 30 individuals per m². A relatively
34
35 305 abundant community of deep-water oysters (100 individuals per m²) is only observed at
36
37 306 a water depth of 744 m at the leeward side of a 1 m high W-E overhanging escarpment.
38
39 307 Here, the top 40 cm underneath the edge is colonized. *Madrepora oculata* was observed
40
41 308 on top of the escarpment’s edge.

42
43
44
45
46
47
48
49 309

50 310 4.2.3 Dive B08-05: Western flank of Guilvinec Canyon

51
52 311 Dive B08-05 mainly investigates the southern shoulder of a gully south of the spur that
53
54
55 312 separates the Guilvinec from the Penmarc’h Canyon (Figs. 1c and 8). The 3100 m long
56
57
58
59
60
61
62
63
64
65

1 313 track followed a southwest course between 300 and 750 m water depth. The overall
2
3 314 gradient of the slope is 8-10°.
4

5
6 315

7
8 316 In contrast with the other dive tracks, this last track does not show a lot of variability in
9
10 317 the encountered facies (Fig. 8). Between 300 and 450 m, the gently dipping slope is
11
12 318 characterized by the presence of straight to gently undulatory sand ripples with a
13
14 319 wavelength between 10 to 15 cm and a general SSE-NNW orientation (Fig. 9a), making
15
16 320 up 37% of the observations. Sometimes coarser sand was observed in between the
17
18 321 ripples. From 450 to 730 m, a relatively flat and bioturbated silty to sandy seafloor is
19
20 322 observed with some small escarpments near 480 m and a low-relief rippled seabed (Fig.
21
22 323 8).
23
24
25
26

27 324

28
29 325 Only at the very end of Dive B08-05, the gentle slope is abruptly interrupted by a large,
30
31 326 laterally continuous 4 m high WSW-ENE rocky escarpment at 735 m. The first meter of
32
33 327 this escarpment is a 50 cm deep overhanging cliff underneath which a thriving
34
35 328 community of *Neopycnodonte zibrowii* oysters, singular *Madrepora oculata* and some
36
37 329 sponges can be observed (Figs. 9b-c). Figure 9d shows the typical high-density
38
39 330 assemblage of *Neopycnodonte zibrowii* which seem to have grown on top of each other.
40
41 331 Their size amounts to 10 cm on the smallest axis and 15 cm on the largest axis. The
42
43 332 density is estimated at 63 individuals per m². Both the oysters as the occasional corals
44
45 333 are hanging “upside down”, concentrated near the most overhanging end of the cliff.
46
47
48
49
50

51 334

52
53
54 335 **5. Discussion**
55
56
57
58
59
60
61
62
63
64
65

1 336 The main part of the discussion is based on the observations made during ROV dive
2
3 337 B06-02 along the La Chapelle continental margin, since it has provided the best
4
5
6 338 overview of the occurrence of *Neopycnodonte zibrowii* in relation with the canyon
7
8 339 environment (Fig. 10). The observations from Guilvinec canyon will be used as
9
10 340 additional information. The habitat in which these giant deep-water oysters are thriving
11
12
13 341 is dependent on both specific morphological and environmental conditions.
14
15
16 342

17 343 ***5.1 The occurrence of deep-water oysters in the Atlantic Ocean***

18 344 These large deep-water oysters (up to 20 cm) belong to the recently described species
19
20 345 *Neopycnodonte zibrowii* (Wisshak et al., 2009a, 2009b), which so far has only been
21
22
23 346 documented alive from the Azores. The use of ROV technology enabled detailed
24
25
26 347 observations of its deep-water habitat in a sheltered environment. Unfortunately, during
27
28
29 348 none of the two R/V Belgica cruises samples could be acquired for morphological or
30
31
32 349 molecular taxonomy. Nevertheless, corresponding alive oysters were observed and
33
34
35 350 sampled with submersible aid at the Azores and were described – together with material
36
37
38 351 recovered during R/V Thalassa expeditions in the early seventies from the southern Bay
39
40 352 of Biscay – as a new species of *Neopycnodonte* by Wisshak et al. (2009b). Previous
41
42 353 observations of mostly dead or sub-fossil specimens were only reported from dredge
43
44
45 354 samples or fisheries by-catch (Le Danois, 1948; Reveillaud et al., 2008). Further
46
47
48 355 isolated records of this species stem from the Gorringe Bank off Portugal (Auzende et
49
50 356 al., 1984), south of Madeira (Hoernle et al., 2001) and in the Central Mediterranean Sea
51
52 357 where they occur as prominent (sub-) fossil oyster banks (Gofas et al., 2007). This
53
54 358 „living fossil’ oyster is most unusual with respect to its habitat, size, geochemical
55
56
57 359 signature and its particularly pronounced centennial longevity (Wisshak et al., 2009a,
58
59
60
61
62
63
64
65

1 360 2009b). It stands in strong contrast to all other extant oyster species which are relatively
2
3 361 short-lived and predominantly occupy shallow to marginal marine settings, where they
4
5 362 occasionally form reefal structures. From the upper slope (200-500 m) of the Bay of
6
7
8 363 Biscay, the related but smaller (4-5 cm) *Neopycnodonte cochlear* has been reported (Le
9
10 364 Danois, 1948). The latter is usually associated with hard substrates and in certain places
11
12 365 colonizes *Dendrophyllia cornigera* coral reefs (Le Danois, 1948). *N. cochlear* certainly
13
14 366 features the largest distribution worldwide, both in palaeo- (Videt and Neraudeau, 2003)
15
16 367 and present-time environments (Harry, 1981). *Neopycnodonte zibrowii*, observed alive
17
18 368 along the La Chapelle continental slope, the Guilvinec Canyon and off the Azores can
19
20 369 be regarded as a distinct deep-sea relative of *N. cochlear* with specific adaptations
21
22 370 allowing it to thrive in upper bathyal depths (now confirmed down to 846 m), and it can
23
24 371 be expected that further direct seabed observations will considerably enhance the known
25
26 372 biogeographic distribution of this unusual bivalved mollusc. Most recently,
27
28 373 Delongueville and Sciallet (2009), reinvestigated two unusually large specimens
29
30 374 sampled alive from the Bay of Biscay margin, previously addressed as *Neopycnodonte*
31
32 375 *cochlear* (Delongueville and Sciallet, 1999), which can now be attributed to
33
34 376 *Neopycnodonte zibrowii*. Interestingly, they were recovered from a water depth of only
35
36 377 350 to 400 m, expanding the known bathymetrical range of this species in the Bay of
37
38 378 Biscay from 350 to 846 metres. In contrast to the Azores, both Biscay pycnodontines
39
40 379 overlap in their bathymetrical range.
41
42
43
44
45
46
47
48
49
50
51

380

381 ***5.2 Influence of the physical environment on deep-water oyster colonization***

382 Up to now, the occurrence of the deep-water oyster *Neopycnodonte zibrowii* within the
383 Bay of Biscay has only been observed on hard substrates. More specifically, the area

1 384 underneath overhanging cliffs, banks or steep escarpments seem to be the most
2
3 385 successful colonization surface (Figs. 5, 9 and 7). This is in contrast with the local
4
5 386 occurrence of other sessile organisms such as cold-water corals (*M. oculata* and *L.*
6
7 387 *pertusa*) and sponges, which are abundantly present on open parts of the slope (Fig. 6).
8
9 388 They have settled on sandy substrate, biogenic debris and on top of elevated substrates,
10
11 389 such as documented for this area by De Mol et al. (accepted) and along the NW
12
13 390 European margin (Dorschel et al., 2009; Freiwald et al., 2004; Huvenne et al., 2005;
14
15 391 Wheeler et al., 2007). Only occasionally, and in reduced numbers, they can be found on
16
17 392 identical substrates colonized by the deep-water oysters (Figs. 7b and 9b). In this case,
18
19 393 such vertical substrates and overhangs could be considered as a challenging surface to
20
21 394 be colonized by cold-water corals. Such specific substrates can be considered as limited
22
23 395 along the continental margins and are specifically concentrated within deep-sea
24
25 396 canyons, where they still are relatively sparsely distributed (less than 5% in this
26
27 397 dataset).
28
29
30
31
32
33
34
35 398
36
37 399 Generally, the morphology of canyons flanks is relatively irregular and no significant
38
39 400 cover of draping sediments is observed. This zone is most likely subject to constant
40
41 401 reworking by downslope (turbiditic) or alongslope (contouritic) current processes
42
43 402 (Arzola et al., 2008; Bourillet et al., 2006; Cunningham et al., 2005; Huthnance, 1995;
44
45 403 Pingree and Le Cann, 1989; Toucanne et al., 2009). Within the depth window
46
47 404 corresponding to the ROV observations, seismic profiles show single, high-amplitude
48
49 405 reflections or diffraction hyperbolae that might indicate the presence of lithified
50
51 406 calcarenite or calcilutites banks (Figs. 3, 10) which possibly belong to the Miocene
52
53 407 Jones or Cockburn Formations (Bourillet et al., 2003; Paquet et al., 2010). Within
54
55
56
57
58
59
60
61
62
63
64
65

1 408 canyons and gullies, predominantly downslope erosion has gradually exposed these
2
3 409 consolidated carbonate-like sedimentary sequences, which have been shaped into step-
4
5
6 410 like banks or escarpments. This process is more intensive towards the centre (thalweg)
7
8 411 of the canyon or gully, providing a higher availability of suitable substrates for
9
10 412 epibenthos colonization (Fig. 10). Evidently, this will also affect the communities of the
11
12 413 sessile organisms that colonize these substrates. If they are too exposed, the epifauna
13
14 414 may be removed by the episodic downslope currents. The overhanging banks and the
15
16 415 vertical escarpments may provide a sufficiently sheltered habitat for the deep-water
17
18 416 oysters, which are capable to settle on such surfaces. However, this particular habitat
19
20 417 does not allow plenty of co-occurring species such as cold-water corals which
21
22 418 necessitate the current exposure. Along the steeper slopes of the La Chapelle continental
23
24 419 slope, relatively more suitable substrates with large deep-water oyster communities
25
26 420 were observed, compared to the Guilvinec area. Moreover, almost no observations were
27
28 421 made of cold-water corals, while they are abundantly present on the gentler Guilvinec
29
30 422 slope (Figs. 4 and 6).
31
32
33
34
35
36
37 423
38
39 424 Additionally, the asymmetry of the Guilvinec Canyon clearly demonstrates a second
40
41 425 factor influencing the location of the deep-water oyster habitats. Both morphologically
42
43 426 and stratigraphically the (north-) western slope of the Guilvinec Canyon shows more
44
45 427 evidence of erosion than the eastern slope, which is characterized by depositional
46
47 428 features (Figs. 1c and 3). ROV observations have shown the presence of seabed ripples
48
49 429 on different parts of this slope between 300 and 950 m (Figs. 6 and 8), suggesting the
50
51 430 presence of an E-W bottom current with velocities between 20 and 40 cm/s (Stow *et al.*,
52
53 431 2009). These observations fit the cyclonic flow circulation and observed depth of the
54
55
56
57
58
59
60
61
62
63
64
65

1 432 MOW in the Bay of Biscay (Fig. 2). The (north-)western slope of the canyon(s) could
2
3 433 act as an obstacle which might intensify the easterly bottom currents through isopycnal
4
5 434 doming, leading to erosion (Hernández-Molina et al., 2003; Iorga and Lozier, 1999; Van
6
7
8 435 Rooij et al., submitted). A similar process was also observed on the upper part of the
9
10 436 Portimao Canyon (Marches et al., 2007). As such, this effect is not present on the
11
12 437 eastern slope, leading to preferential deposition on this side of the canyon, making it
13
14 438 nearly devoid of banks and escarpments. This example also proves that a combined
15
16 439 influence of turbiditic and contouritic currents may shape the canyon morphology and
17
18 440 hence determine the location of preferential habitats of (hidden) deep-water ecosystems.
19
20
21 441 Both the banks as the cliffs will not easily be subject to sediment burial and provide a
22
23 442 suitable hard substrate for this type of filter feeders. As such, there is not much
24
25 443 competition between the deep-water oysters and cold-water corals, since they seem to
26
27 444 have slightly different physical habitat requirements.
28
29
30
31
32
33
34

35 446 ***5.3 Oceanographic drivers for deep-water oyster occurrence***

36
37 447 Next to the necessary settling grounds, a successful oyster habitat needs the suitable
38
39 448 oceanographic environment and sufficient nutrients. During some of the ROV dives, an
40
41 449 intense marine snow was present in the area where the oyster community was
42
43 450 discovered (Figs. 5a, 7c-d and 9c). This aggregated particulate matter composed of
44
45 451 phytodetritus and pellets, sinking from the upper water layers, constitutes an important
46
47 452 aspect in the trophic input of this community. Oysters are filter feeders, commonly
48
49 453 located in low salinity coastal shallow water and feeding on phytoplankton. The
50
51 454 occurrence of oysters at these depths is at least remarkable given the higher salinities
52
53 455 and generally lower input of phytodetritus. On the other hand, a relatively high surface
54
55
56
57
58
59
60
61
62
63
64
65

1 456 primary production is present along this part of the margin (Joint et al., 2001; Pingree
2
3 457 and Le Cann, 1990). Moreover, according to the available hydrographic data, the depth
4
5 458 range in which *Neopycnodonte zibrowii* is observed lies just beneath the physical
6
7
8 459 boundary between the upper Eastern North Atlantic Water and the intermediate saline
9
10 460 Mediterranean Outflow Water (Fig. 2). The lower limit of the oyster's occurrence
11
12 461 coincides with a local salinity and temperature maximum of respectively 35.75 and
13
14 462 10°C, which might indicate a certain amount mixing of both water masses. Within this
15
16 463 zone of upper MOW, seabed features indicate a locally vigorous hydrodynamic
17
18 464 environment near the gully shoulders (Figs. 4, 6 and 8). The observations of straight
19
20 465 sand ripples during dive B06-02 indicate the presence of strong bottom currents
21
22 466 between 10 and 40 cm/s (Stow et al., 2009). Apart from the flow velocity of the MOW,
23
24 467 the bottom currents may be enhanced by strong internal tides (White, 2007) and
25
26 468 funnelled along the canyon axis, as observed in the Portimao Canyon (Marches et al.,
27
28 469 2007). This is consistent with previous measurements along the Armorican margin
29
30 470 (Pingree and Le Cann, 1989, 1990), where a strongest bottom current near the 500 m
31
32 471 contour was observed in the downslope direction with a maximum instantaneous
33
34 472 velocity of 95 cm/s. Intersected with canyons, these tidally induced transports may be
35
36 473 channelled and result in regions of locally increased flow, resuspension and local
37
38 474 circulations (Pingree and Le Cann, 1990). A dominant effect caused by internal tides
39
40 475 from the upper slope is proposed to explain the entrapment and downward transport of
41
42 476 the enhanced levels of surface phytoplankton abundance (Holligan et al., 1985; Pingree
43
44 477 et al., 1982) as recently inferred above the Nazaré Canyon (Arzola et al., 2008) and
45
46 478 above giant carbonate mound provinces colonised by reef-forming cold-water corals
47
48 479 (Mienis et al., 2007; White, 2007) . The significance of submarine canyons as coral and
49
50
51
52
53
54
55
56
57
58
59
60
61
62
63
64
65

1 480 oyster habitats (Mortensen and Buhl-Mortensen, 2005) may be due to their capacity to
2
3 481 accumulate organic debris (Canals et al., 2006), which may directly benefit filter-
4
5 482 feeders, such as scleractinians (Roberts et al., 2006). It is highly likely that this water-
6
7 483 mixing above the seabed results in enhanced suspended material and favours
8
9 484 concentration of filter/suspension feeders (de Stigter et al., 2007).

10
11 485
12
13
14
15 486 Moreover, the oyster banks occur in a potential density envelope of 27.4 – 27.7 kg/m³
16
17 487 (Fig. 2), overlapping the range of values which are considered to be a prerequisite for
18
19 488 the development, growth and distribution of cold-water coral reefs along the Celtic and
20
21 489 Nordic European margin (Dullo et al., 2008) and within the Guilvinec area (De Mol et
22
23 490 al., accepted). This control through potential density may be linked to the formation of
24
25 491 intermediate nepheloid layers, which increase nutrient supply and resuspension (de
26
27 492 Stigter et al., 2007; Mienis et al., 2007). As such, in contrast to the shallow marine
28
29 493 oyster occurrences, the dynamic oceanography within deep-sea canyons can provide a
30
31 494 stable ecosystem which enables a theoretical co-habitation with sponges, hydrozoans,
32
33 495 gorgonians and scleractinians (De Mol et al., accepted).

34
35
36
37
38
39
40 496

41 42 497 **6. Conclusions**

43
44 498 In this paper, the occurrence and the environmental drivers of a hidden deep-water
45
46 499 habitat (540-846 m), inhabited by *Neopycnodonte zibrowii* oysters along the French
47
48 500 Atlantic continental margin, is described. The present observations indicate that canyons
49
50 501 and steep slopes may provide the most suitable physical environment for these oysters,
51
52 502 which are predominantly observed underneath overhanging banks or on escarpments.
53
54 503 Turbiditic and contouritic processes are responsible for (1) the erosion which exposes
55
56
57
58
59
60
61
62
63
64
65

1 504 consolidated carbonate-like sedimentary sequences, shaping them into step-like banks,
2
3 505 and (2) the delivery and resuspension of nutrients in association with funnelling of
4
5 506 internal tides into canyons. Although these deep-water oysters occur in a similar
6
7
8 507 oceanographic setting as cold-water corals, their very specific physical habitat
9
10 508 requirements do not seem to be fully compatible with most of the other sessile
11
12 509 organisms. Once these rather strict and sparsely distributed environments are
13
14 510 encountered, *Neopycnodonte zibrowii* can be observed in relatively high number up to
15
16 511 100 individuals per m².
17
18
19
20
21 512

22
23 513 This little-known population located in an inaccessible environment sheds light on the
24
25 514 richness of canyon systems in terms of filter feeder species. Because of the verticality of
26
27 515 this habitat, acoustic hull-mounted systems and bottom sampling with conventional
28
29 516 towed devices will be unsuitable for a fine description of this population. As such,
30
31 517 further in situ observations and habitat mapping from ROV's should be performed to
32
33 518 estimate the oyster coverage along the Bay of Biscay and other Atlantic canyons. They
34
35 519 may represent an overlooked deep-water community, being part of a still vastly
36
37 520 underestimated biodiversity of bathyal benthic communities, especially within canyons.
38
39
40
41
42
43

44 521

45 522 **Acknowledgements**

46
47 523 This research was supported by the HERMES project (EC contract n° GOCE-CT-
48
49 524 2005-511234), funded by the European Commission's Sixth Framework Programme
50
51 525 under the priority 'Sustainable Development, Global Change and Ecosystems' and by
52
53 526 ESF EuroDIVERSITY MiCROSYSTEMS (05_EDIV_FP083-MiCROSYSTEMS). A
54
55 527 follow-up of this research will be performed within the framework of the EC FP7 IP
56
57
58
59
60
61
62
63
64
65

1 528 HERMIONE project (grant agreement n° 226354). We are indebted to the entire ROV
2
3 529 *Genesis* technical team of Ghent University (Belgium). The captains, crews and
4
5
6 530 shipboard scientific parties of the R/V Belgica ST0612 and ST0813a campaigns are also
7
8 531 acknowledged for their enthusiastic efforts. We are grateful to Dr. L. Chou (ULB,
9
10 532 Belgium) for kindly providing CTD data (Station 3 cast B). The authors also kindly
11
12 533 acknowledge H. Pirlet, in addition to 4 anonymous reviewers, for the useful comments
13
14 534 and suggestions which helped improving this manuscript. LDM acknowledges the
15
16 535 support through an IWT-grant. The research of DVR was funded through an FWO
17
18 536 Flanders post-doctoral fellowship.
19
20
21
22
23
24

25 538 **Appendix A. Supplementary material**

26
27 539 Supplementary data associated with this article can be found in the online version at...

30 540

31 541 **References**

- 32
33
34
35 542 Arzola, R.G., Wynn, R.B., Lastras, G., Masson, D.G., Weaver, P.P.E., 2008.
36
37 543 Sedimentary features and processes in the Nazaré and Setúbal submarine
38
39 544 canyons, west Iberian margin. *Marine Geology*, 250(1-2), 64-88.
40
41
42 545 Auzende, J.-M., Charvet, J., Le Lann, A., Le Pichon, X., Monteiro, J.-H., Nicolas, A.,
43
44 546 Olivet, J.-L., Ribeiro, A., 1984. *Géologie du Banc de Gorringe, Campagne*
45
46 547 *CYAGOR II. Résultats des Campagnes à la Mer 27. Publications du Centre*
47
48 548 *National pour l'Exploration des Océans (CNEXO), Brest, 65 pp.*
49
50
51 549 Botas, J.A., Fernández, E., Bode, A., Anadón, R., 1989. Water masses off central
52
53 550 Cantabrian coast. *Scientia Marina*, 53, 755-761.
54
55
56
57
58
59
60
61
62
63
64
65

1 551 Bourillet, J.F., Reynaud, J.Y., Baltzer, A., Zaragosi, S., 2003. The 'Fleuve Manche': the
2
3 552 submarine sedimentary features from the outer shelf to the deep-sea fans.
4
5
6 553 Journal of Quaternary Science, 18(3-4), 261-282.
7
8 554 Bourillet, J.F., Zaragosi, S., Mulder, T., 2006. The French Atlantic margin and deep-sea
9
10 555 submarine systems. Geo-Marine Letters, 26(6), 311-315.
11
12 556 Canals, M., Puig, P., de Madron, X.D., Heussner, S., Palanques, A., Fabres, J., 2006.
13
14 557 Flushing submarine canyons. Nature, 444(7117), 354-357.
15
16
17 558 Cunningham, M.J., Hodgson, S., Masson, D.G., Parson, L.M., 2005. An evaluation of
18
19 559 along- and down-slope sediment transport processes between Goban Spur and
20
21 560 Brenot Spur on the Celtic Margin of the Bay of Biscay. Sedimentary Geology,
22
23 561 179, 99-116.
24
25
26 562 Delongueville, C., Sciallet, R. 1999. *Neopycnodonte cochlear* (Poli, 1795) dans le Golfe
27
28 563 de Gascogne. Arion 24(2), 62
29
30
31 564 Delongueville, C., Sciallet, R. 2009. *Neopycnodonte zibrowii* Gofas, Salas & Taviani in
32
33 565 Wisshak *et al.*, 2009 dans le golfe de Gascogne. Novapex 10(1), 9-12.
34
35
36 566 De Mol, L., Van Rooij, D., Pirlet, H., Greinert, J., Frank, N., Quemmerais, F., Henriet,
37
38 567 J.P., the R/V Belgica 08/13a shipboard scientific party, accepted. Cold-water
39
40 568 coral habitats in the Penmarc'h and Guilvinec canyons (Bay of Biscay): deep-
41
42 569 water versus shallow water settings. Marine Geology.
43
44
45 570 de Stigter, H., Boer, W., de Jesus Mendes, P.A., Jesus, C.C., Thomsen, L., van den
46
47 571 Bergh, G.D., van Weering, T.C.E., 2007. Recent sediment transport and
48
49 572 deposition in the Nazaré Canyon, Portuguese continental margin. Marine
50
51 573 Geology, 246, 144-164.
52
53
54
55
56
57
58
59
60
61
62
63
64
65

1 574 Dorschel, B., Wheeler, A.J., Huvenne, V.A.I., de Haas, H., 2009. Cold-water coral
2
3 575 mounds in an erosive environmental setting: TOBI side-scan sonar data and
4
5 576 ROV video footage from the northwest Porcupine Bank, NE Atlantic. *Marine*
6
7
8 577 *Geology*, 264(3-4), 218-229.
9
10 578 Duineveld, G., Lavaleye, M., Berghuis, E., de Wilde, P., 2001. Activity and
11
12 579 composition of the benthic fauna in the Whittard Canyon and the adjacent
13
14 580 continental slope (NE Atlantic). *Oceanologica Acta*, 24(1), 69-83.
15
16
17 581 Dullo, C., Flögel, S., Rüggeberg, A., 2008. Cold-water coral growth in relation to the
18
19 582 hydrography of the Celtic and Nordic European continental margin. *Marine*
20
21 583 *Ecology Progress Series*, 371, 165-176.
22
23
24 584 Freiwald, A., Fossa, J.H., Grehan, A., Koslow, T., Roberts, J.M., 2004. Cold-water
25
26 585 coral reefs. *Biodiversity Series*. UNEP-WCMC, Cambridge, 84 pp.
27
28
29 586 Gofas, S., Freiwald, A., López Correa, M., Remia, A., Salas, C., Taviani, M., Wisshak,
30
31 587 M., Zibrowius, H., 2007. Oyster beds in the deep sea. In: K. Jordaens, N. van
32
33 588 Houtte, J. van Goethem, T. Backeljau (Eds), *World Congress of Malacology*,
34
35 589 Antwerp, Belgium, pp. 80.
36
37
38 590 Halpern, B.S., Walbridge, S., Selkoe, K.A., Kappel, C.V., Micheli, F., D'Agrosa, C.,
39
40 591 Bruno, J.F., Casey, K.S., Ebert, C., Fox, H.E., Fujita, R., Heinemann, D.,
41
42 592 Lenihan, H.S., Madin, E.M.P., Perry, M.T., Selig, E.R., Spalding, M., Steneck,
43
44 593 R., Watson, R., 2008. A global map of human impact on marine ecosystems.
45
46 594 *Science*, 319(5865), 948-952.
47
48
49 595 Harry, H.W., 1981. Nominal species of living oysters proposed during the last fifty
50
51 596 years. *Veliger*, 24, 39-45.
52
53
54
55
56
57
58
59
60
61
62
63
64
65

1 597 Haynes, R., Barton, 1990. A poleward flow along the Atlantic coast of the Iberian
2
3 598 Peninsula. *Journal of Geophysical Research*, 95, 11425-11441.
4
5 599 Hernández-Molina, J., Llave, E., Somoza, L., Fernandez-Puga, M.C., Maestro, A.,
6
7 600 Leon, R., Medialdea, T., Barnolas, A., Garcia, M., del Rio, V.D., Fernandez-
8
9 601 Salas, L.M., Vazquez, J.T., Lobo, F., Dias, J.M.A., Rodero, J., Gardner, J., 2003.
10
11 602 Looking for clues to paleoceanographic imprints: A diagnosis of the Gulf of
12
13 603 Cadiz contourite depositional systems. *Geology*, 31(1), 19-22.
14
15
16
17 604 Hoernle, K., Shipboard party, 2001. METEOR Cruise No. M51, Leg 1, VULKOSO -
18
19 605 Vulkanismus Ostatlantik-Alboran. GEOMAR, Bremen, 94 pp.
20
21
22 606 Holligan, P.M., Pingree, R.D., Mardell, G.T., 1985. Oceanic Solitions, Nutrient Pulses
23
24 607 and Phytoplankton Growth. *Nature*, 314(6009), 348-350.
25
26
27 608 Huetten, E., Greinert, J., 2008. Software controlled guidance, recording and post-
28
29 609 processing of seafloor observations by ROV and other towed devices: the
30
31 610 software package OFOP. *Geophysical Research Abstracts*, 10, EGU2008-A-
32
33 611 03088.
34
35
36
37 612 Huthnance, J.M., 1995. Circulation, exchange and water masses at the ocean margin:
38
39 613 the role of physical processes at the shelf edge. *Progress in Oceanography*, 35,
40
41 614 353-431.
42
43
44 615 Huvenne, V., Beyer, A., de Haas, H., Dekindt, K., Henriët, J.P., Kozachenko, M., Olu-
45
46 616 Le Roy, K., Wheeler, A., the TOBI/Pelagia 197 and CARACOLE cruise
47
48 617 participants, 2005. The seabed appearance of different coral bank provinces in
49
50 618 the Porcupine Seabight, NE Atlantic: results from sidescan sonar and ROV
51
52 619 seabed mapping. In: A. Freiwald, J.M. Roberts (Eds.), *Cold-water Corals and*
53
54 620 *Ecosystems*. Springer-Verlag, Berlin Heidelberg, pp. 535-569.
55
56
57
58
59
60
61
62
63
64
65

1 621 Iorga, M.C., Lozier, M.S., 1999. Signatures of the Mediterranean outflow from a North
2
3 622 Atlantic climatology 1. Salinity and density fields. *Journal of Geophysical*
4
5 623 *Research-Oceans*, 104(C11), 25985-26009.

6
7
8 624 IPCC, 2007. *Climate Change 2007: The Physical Science Basis. Contribution of*
9
10 625 *Working Group I to the Fourth Assessment Report of the Intergovernmental*
11
12 626 *Panel on Climate Change. Cambridge University Press, Cambridge, 996 pp.*

13
14
15 627 Joint, I., Wollast, R., Chou, L., Batten, S., Elskens, M., Edwards, E., Hirst, A., Burkill,
16
17 628 P., Groom, S., Gibb, S., Miller, A., Hydes, D., Dehairs, F., Antia, A., Barlow,
18
19 629 R., Rees, A., Pomroy, A., Brockmann, U., Cummings, D., Lampitt, R., Loijens,
20
21 630 M., Mantoura, F., Miller, P., Raabe, T., Alvarez-Salgado, X., Stelfox, C.,
22
23 631 Woolfenden, J., 2001. Pelagic production at the Celtic Sea shelf break. *Deep Sea*
24
25 632 *Research Part II: Topical Studies in Oceanography*, 48(14-15), 3049-3081.

26
27
28
29 633 Le Danois, E., 1948. *Les profondeurs de la mer. Payot, Paris, 303 pp.*

30
31
32 634 Marches, E., Mulder, T., Cremer, M., Bonnel, C., Hanquiez, V., Gonthier, E., Lecroart,
33
34 635 P., 2007. Contourite drift construction influenced by capture of Mediterranean
35
36 636 Outflow Water deep-sea current by the Portimao submarine canyon (Gulf of
37
38 637 Cadiz, South Portugal). *Marine Geology*, 242(4), 247-260.

39
40
41
42 638 McCartney, M.S., 1992. Recirculating components to the deep boundary current of the
43
44 639 northern North Atlantic. *Progress in Oceanography*, 29, 283-383.

45
46
47 640 McCave, I.N., Hall, I.R., Antia, A.N., Chou, L., Dehairs, F., Lampitt, R.S., Thomsen,
48
49 641 L., van Weering, T.C.E., Wollast, R., 2001. Distribution, composition and flux
50
51 642 of particulate material over the European margin at 47°-50°N. *Deep-Sea*
52
53 643 *Research II*, 48, 3107-3139.

54
55
56
57
58
59
60
61
62
63
64
65

- 1 644 Mienis, F., de Stigter, H., White, M., Duineveld, G.C.A., de Haas, H., van Weering, T.,
2
3 645 2007. Hydrodynamic controls on cold-water coral growth and carbonate-mound
4
5 646 development at the SW and SE Rockall Trough Margin, NE Atlantic Ocean.
6
7
8 647 Deep-Sea Research I, 54, 1655-1674.
9
- 10 648 Mortensen, P., Buhl-Mortensen, L., 2005. Deep-water corals and their habitats in The
11
12 649 Gully, a submarine canyon off Atlantic Canada. In: A. Freiwald, J.M. Roberts
13
14 650 (Eds.), Cold-Water Corals and Ecosystems. Springer-Verlag, Berlin Heidelberg,
15
16 651 pp. 247-277.
17
18
19 652 Pairaud, I.L., Lyard, F., Auclair, F., Letellier, T., Marsaleix, P., 2008. Dynamics of the
20
21 653 semi-diurnal and quarter-diurnal internal tides in the Bay of Biscay. Part 1:
22
23 654 Barotropic tides. Continental Shelf Research, 28(10-11), 1294-1315.
24
25
26 655 Palanques, A., Puig, P., Latasa, M., Scharek, R., 2009. Deep sediment transport induced
27
28 656 by storms and dense shelf-water cascading in the northwestern Mediterranean
29
30 657 basin. Deep-Sea Research I, 56(3), 425-434.
31
32
33 658 Paquet, F., Menier, D., Estournès, G., Bourillet, J.-F., Leroy, P., Guillocheau, F., 2010.
34
35 659 Buried fluvial incisions as a record of Middle-Late Miocene eustasy fall on the
36
37 660 Armorican Shelf (Bay of Biscay, France). Marine Geology, 268(1-4), 137-151.
38
39
40 661 Pingree, R.D., Le Cann, B., 1989. Celtic and Armorican slope and shelf residual
41
42 662 currents. Progress in Oceanography, 23, 303-338.
43
44
45 663 Pingree, R.D., Le Cann, B., 1990. Structure, strength and seasonality of the slope
46
47 664 currents in the Bay of Biscay region. Journal of the Marine Biological
48
49 665 Association of the United Kingdom, 70, 857-885.
50
51
52
53
54
55
56
57
58
59
60
61
62
63
64
65

1 666 Pingree, R.D., Le Cann, B., 1992. Three anticyclonic Slope Water Oceanic eDDIES
2
3 667 (SWODDIES) in the southern Bay of Biscay in 1990. *Deep-Sea Research*, 39,
4
5 668 1147-1176.
6
7
8 669 Pingree, R.D., Mardell, G.T., Holligan, P.M., Griffiths, D.K., Smithers, J., 1982. Celtic
9
10 670 Sea and Armorican Current Structure and the Vertical Distributions of
11
12 671 Temperature and Chlorophyll. *Continental Shelf Research*, 1(1), 99-116.
13
14
15 672 Pollard, S., Griffiths, C.R., Cunningham, S.A., Read, J.F., Perez, F.F., Ríos, A.F., 1996.
16
17 673 Vivaldi 1991 - A study of the formation, circulation and ventilation of Eastern
18
19 674 North Atlantic Central Water. *Progress in Oceanography*, 37, 167-192.
20
21
22 675 Reveillaud, J., Freiwald, A., Van Rooij, D., Le Guilloux, E., Altuna, A., Foubert, A.,
23
24 676 Vanreusel, A., Roy, K.O.L., Henriët, J.P., 2008. The distribution of scleractinian
25
26 677 corals in the Bay of Biscay, NE Atlantic. *Facies*, 54(3), 317-331.
27
28
29 678 Roberts, J.M., Wheeler, A.J., Freiwald, A., 2006. Reefs of the Deep: The Biology and
30
31 679 Geology of Cold-Water Coral Ecosystems. *Science*, 312(5773), 543-547.
32
33
34 680 Stow, D.A.V., Hernández-Molina, F.J., Llave, E., Sayago-Gil, M., del Rio, V.D.,
35
36 681 Branson, A., 2009. Bedform-velocity matrix: The estimation of bottom current
37
38 682 velocity from bedform observations. *Geology*, 37(4), 327-330.
39
40
41 683 Toucanne, S., Zaragosi, S., Bourillet, J.F., Cremer, M., Eynaud, F., Van Vliet-Lanoë,
42
43 684 B., Penaud, A., Fontanier, C., Turon, J.L., Cortijo, E., Gibbard, P.L., 2009.
44
45 685 Timing of massive 'Fleuve Manche' discharges over the last 350 kyr: insights
46
47 686 into the European ice-sheet oscillations and the European drainage network from
48
49 687 MIS 10 to 2. *Quaternary Science Reviews*, 28(13-14), 1238-1256.
50
51
52 688 Van Aken, H.M., 2000. The hydrography of the mid-latitude Northeast Atlantic Ocean
53
54 689 II: The intermediate water masses. *Deep-Sea Research I*, 47, 789-824.
55
56
57
58
59
60
61
62
63
64
65

1 690 Van Rooij, D., Iglesias, J., Hernández-Molina, F.J., Ercilla, G., Gomez-Ballesteros, M.,
2
3 691 Casas, D., Llave, E., De Hauwere, A., Garcia-Gil, S., Acosta, J., Henriët, J.-P.,
4
5
6 692 submitted. The Le Danois Contourite Depositional System: interactions between
7
8 693 the Mediterranean Outflow Water and the upper Cantabrian slope (North Iberian
9
10 694 margin). *Marine Geology*.

11
12 695 Vangriesheim, A., Khripounoff, A., 1990. Near-bottom particle concentration and flux:
13
14
15 696 Temporal variations observed with sediment traps and nephelometer on the
16
17
18 697 Meriadzek Terrace, Bay of Biscay. *Progress In Oceanography*, 24(1-4), 103-116.

19
20 698 Videt, B., Neraudeau, D., 2003. Variability and heterochronies of *Rhynchostreon*
21
22 699 *suborbiculatum* (Lamarck, 1801) (Bivalvia : Ostreoidea : Gryphaeidae :
23
24
25 700 Exogyrinae) from the Cenomanian and the Lower Taronian of Charentes (SW
26
27
28 701 France). *Comptes Rendus Palevol*, 2(6-7), 563-576.

29
30 702 Weaver, P.P.E., Gunn, V., 2009. INTRODUCTION TO THE SPECIAL ISSUE
31
32 703 HERMES Hotspot Ecosystem Research on the Margins of European Seas.
33
34
35 704 *Oceanography*, 22(1), 12-15.

36
37 705 Wessel, P., Smith, W.H.F., 1991. Free Software helps Map and Display Data. *EOS*
38
39
40 706 *Transactions AGU*, 72(441), 445-446.

41
42 707 Wheeler, A.J., Beyer, A., Freiwald, A., de Haas, H., Huvenne, V.A.I., Kozachenko, M.,
43
44
45 708 Olu-Le Roy, K., Opderbecke, J., 2007. Morphology and environment of cold-
46
47
48 709 water coral carbonate mounds on the NW European margin. *International*
49
50 710 *Journal of Earth Sciences*, 96, 37-56.

51
52 711 White, M., 2007. Benthic dynamics at the carbonate mound regions of the Porcupine
53
54
55 712 Sea Bight continental margin. *International Journal of Earth Sciences*, 96, 1-9.

1 713 Wienberg, C., Hebbeln, D., Fink, H.G., Mienis, F., Dorschel, B., Vertino, A., Correa,
2
3 714 M.L., Freiwald, A., 2009. Scleractinian cold-water corals in the Gulf of Cádiz--
4
5 715 First clues about their spatial and temporal distribution. Deep Sea Research I,
6
7
8 716 56(10), 1873-1893.
9
10 717 Wisshak, M., López Correa, M., Gofas, S., Salas, C., Taviani, M., Jakobsen, J.,
11
12 718 Freiwald, A., 2009a. Shell architecture, element composition, and stable isotope
13
14 719 signature of the giant deep-sea oyster *Neopycnodonte zibrowii* sp. n. from the
15
16 720 NE Atlantic. Deep Sea Research I, 56(3), 374-407.
17
18 721 Wisshak, M., Neumann, C., Jakobsen, J., Freiwald, A., 2009b. The 'living-fossil
19
20 722 community' of the cyrtocrinid *Cyathidium foresti* and the deep-sea oyster
21
22 723 *Neopycnodonte zibrowii* (Azores Archipelago). Palaeogeography,
24
25 724 Palaeoclimatology, Palaeoecology, 271(1-2), 77-83.
26
27 725 Zaragosi, S., Auffret, G.A., Faugères, J.-C., Garlan, T., Pujol, C., Cortijo, E., 2000.
28
29 726 Physiography and recent sediment distribution of the Celtic Deep-Sea Fan, Bay
30
31 727 of Biscay. Marine Geology, 169, 207-237.
32
33
34
35
36
37
38
39

40 **Tables**

41
42 730 Table 1: Metadata of the ROV Genesis dive tracks
43
44

Dive name & Date	Location	Start		End		Oyster depth
		Coordinates	Time & Depth	Coordinates	Time & Depth	
B06-02 17 June 2006	East flank Ostrea Spur	47°33.34'N 7°20.69'W	08:31 587 m	47°34.07'N 7°19.44'W	15:25 557 m	540 – 680 m

B08-02	North-western	46°56.27'N	11:24	46°55.72'N	15:46	720 –
1 June	flank	5°22.89'W	712 m	5°22.90'W	900 m	846 m
2008	Guilvinec Canyon					
B08-05	Western flank	46°55.68'N	11:17	46°55.16'N	14:27	737 -
3 June	Guilvinec	5°28.52'W	305 m	5°29.00'W	737 m	740 m
2008	Canyon					

731

732 Table 2: Metadata of the CTD casts

Name	Date	Location	Latitude	Longitude	Depth
Station 3 cast B	1 June 2006	La Chapelle slope	47°25.00'N	7°16.00' W	1396 m
B0813-CTD-4	4 June 2008	Guilvinec canyon	46°54.53'N	5°21.26'W	1404 m

733

734 **Figure captions**

735

736 Figure 1: (a). Location of the study areas along the French Atlantic continental margin
737 (GEBCO bathymetry, contour lines every 250 m), with indication of the CTD locations
738 (Table 2) and of the historical *Massifs Coralliens* mapped by Le Danois (1948); MCBC:
739 *Massif Corallien du Banc de la Chapelle*; MBP; *Massif Corallien du Sud Ouest de*
740 *Penmarc'h*; MCGV; *Massif Corallien de la Grande Vasière*. (b). Detail of the Ostrea
741 Spur area with EM1002 bathymetry (contour spacing 25 m) and the location of ROV
742 dive B06-02 (white). (c). Detail of the Guilvinec Canyon area with EM1002 bathymetry
743 (contour spacing 25 m), with the location of seismic profiles (red) and ROV dives B08-
744 02 and B08-05 (white).

1 745
2
3 746 Figure 2: Hydrographic data of the two study areas. (a). Temperature/salinity plot for
4
5 747 both CTD casts (Table 2), with indication of the boundary (dashed grey line) between
6
7 748 the Eastern North Atlantic Water (ENAW) and the Mediterranean Outflow Water
8
9 749 (MOW). The red and blue dashed envelopes refer to the occurrence of cold-water coral
10
11 750 (CWC) reefs in respectively the Porcupine Seabight (Dullo et al., 2008) and within the
12
13 751 Guilvinec canyon (De Mol et al., accepted). The estimated occurrence envelope of
14
15 752 deep-water oysters in the Bay of Biscay is based on the ROV observations (Table 1),
16
17 753 plotted on the CTD data of respectively (b) cast “Station 3 cast B” and (c) cast “B0813-
18
19 754 CTD-4” in full grey. Here, the black vertical bars indicate the corresponding depth
20
21 755 range of ROV observations.
22
23
24
25
26
27

28 756
29
30 757 Figure 3: Seismic profiles Ga080605 (A) and Ga080604 (B), illustrating the seismic
31
32 758 stratigraphy and thickness of the sedimentary cover across the Guilvinec Canyon (Fig.
33
34 759 1c). Note the asymmetry of canyon morphology and the difference between the
35
36 760 sedimentary processes on both flanks. The white dashed lines indicated additional
37
38 761 unconformities within the main sequences. These figures have a 10 times vertical
39
40 762 exaggeration.
41
42
43
44

45 763
46
47 764 Figure 4: ROV dive B06-02 track superimposed on the R/V Belgica EM1002
48
49 765 bathymetry (contour lines every 50 m) with indication of the recognized lithologies,
50
51 766 seabed features and the location of the imagery shown in Fig. 5. The black trackline
52
53 767 represents a featureless, sandy bioturbated seabed.
54
55
56

57 768
58
59
60
61
62
63
64
65

1 769 Figure 5: Video-derived images of oyster assemblages and facies recognized during
2
3 770 dive B06-02 (Fig. 4). Each image bears depth information and orientation. (a) NW-SE
4
5 771 straight sand ripples, (b) carbonate knolls with *Hexadella* sp. sponge, (c) carbonate
6
7 772 banks in a series of steps, (d) overhanging carbonate bank with (low-density) oyster
8
9 773 community attached below the bank, in association with a dead cold-water coral, (e)
10
11 774 close-up of a probably living (high density) deep-water oyster community, (f) steep
12
13 775 oyster cliff, note the altitude of the ROV (5.3 m above sea floor).
14
15
16
17

18 776
19
20 777 Figure 6: ROV dive B08-02 track superimposed on the R/V Belgica EM1002
21
22 778 bathymetry (contour lines every 50 m) with indication of the recognized lithologies,
23
24 779 seabed features and the location of the stills imagery shown in Fig. 7. The black
25
26 780 trackline represents a featureless, silt-sandy bioturbated seabed.
27
28
29

30 781
31
32 782 Figure 7: Stills images of oyster assemblages and facies recognized during dive B08-02
33
34 783 (Fig. 6); (a) E-W escarpment (± 3 m high) with frequent oyster colonization, (b), S-N
35
36 784 oriented escarpment with a mixed solitary oyster and cold-water coral community
37
38 785 (*Lophelia pertusa*, black corals (*Parantipathes* sp., *Stichopathes* sp., *Trissopathes* sp.),
39
40 786 (c) undulatory S-N oriented sand ripples with sparse live solitary *Madrepora oculata*,
41
42 787 (d) leeward side of a W-E outcropping and overhanging rock (± 1 m high), colonized by
43
44 788 deep-water oysters.
45
46
47
48

49 789
50
51 790 Figure 8: ROV dive B08-05 track superimposed on the R/V Belgica EM1002
52
53 791 bathymetry (contour lines every 50 m) with indication of the recognized lithologies,
54
55
56
57
58
59
60
61
62
63
64
65

1 792 seabed features and the location of the stills imagery shown in Fig. 9. The black
2
3 793 trackline represents a featureless, silty-sandy bioturbated seabed.
4
5
6 794
7
8 795 Figure 9: Stills images of oyster assemblages and facies recognized during dive B08-05
9
10 796 (Fig. 8); (a) undulatory SSE-NNW oriented sand ripple field and the fish *Chimera*
11
12 797 *monstrosa* and *Helicolenus dactylopterus dactylopterus*, (b) overhanging cliff with a
13
14 798 thriving mixed oyster and *Madrepora oculata* colony, (c) distant view of a S-N
15
16 799 colonized overhanging cliff, (d) detailed view of the densely packed deep-water oyster
17
18 800 community.
19
20
21 801
22
23 802 Figure 10: Conceptual sketch of the deep-water oyster environment, based on ROV dive
24
25 803 B06-02 on the La Chapelle continental slope. The main oyster communities are located
26
27 804 at the gully axis, fed by cascading currents enabling a suitable nutrient supply. The
28
29 805 banks upon which the oysters are seated probably are Miocene carbonate banks
30
31 806 (calcarenites).
32
33
34
35
36
37
38
39
40
41
42
43
44
45
46
47
48
49
50
51
52
53
54
55
56
57
58
59
60
61
62
63
64
65

Figure 01

[Click here to download high resolution image](#)

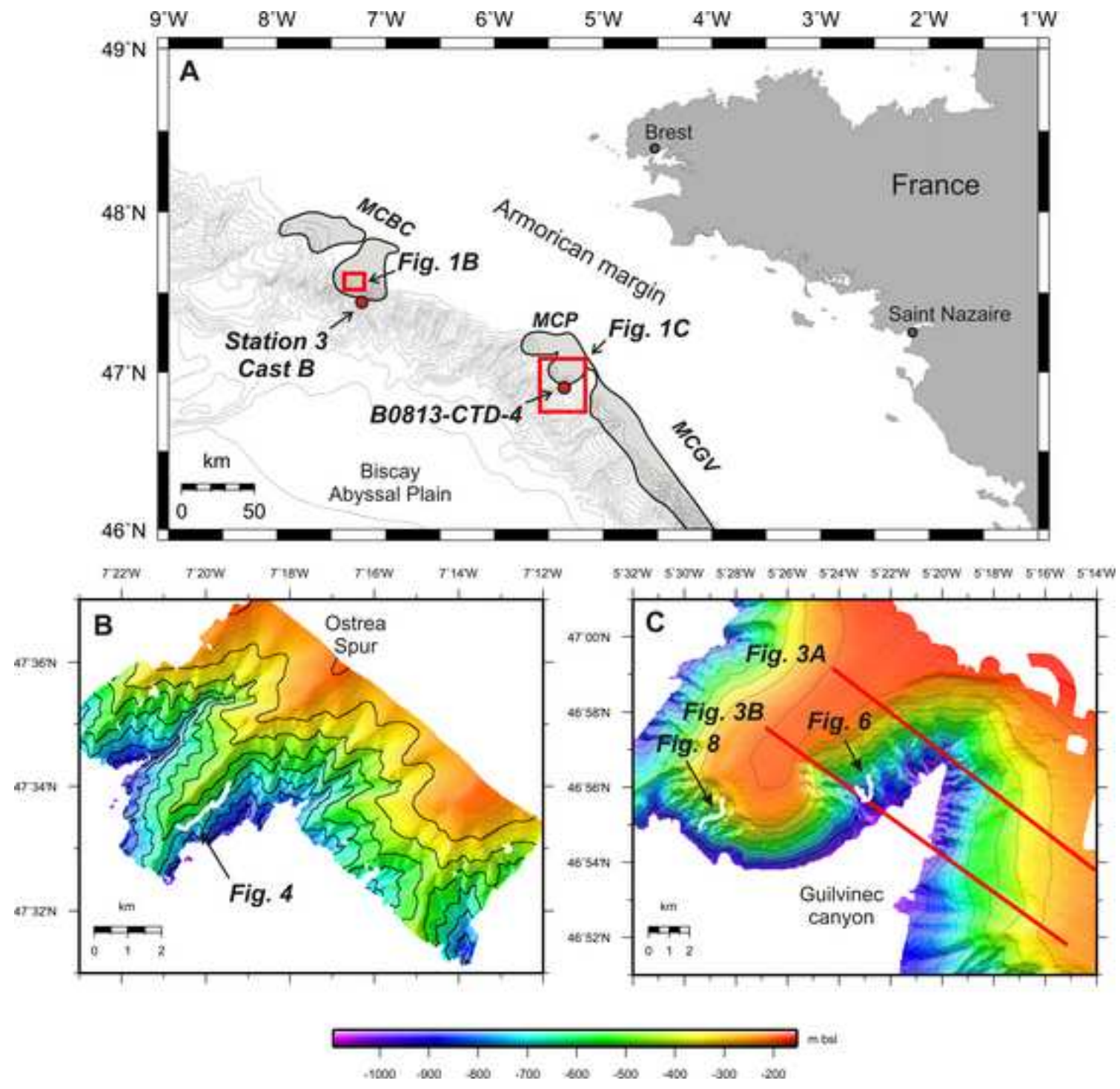


Figure 02
[Click here to download high resolution image](#)

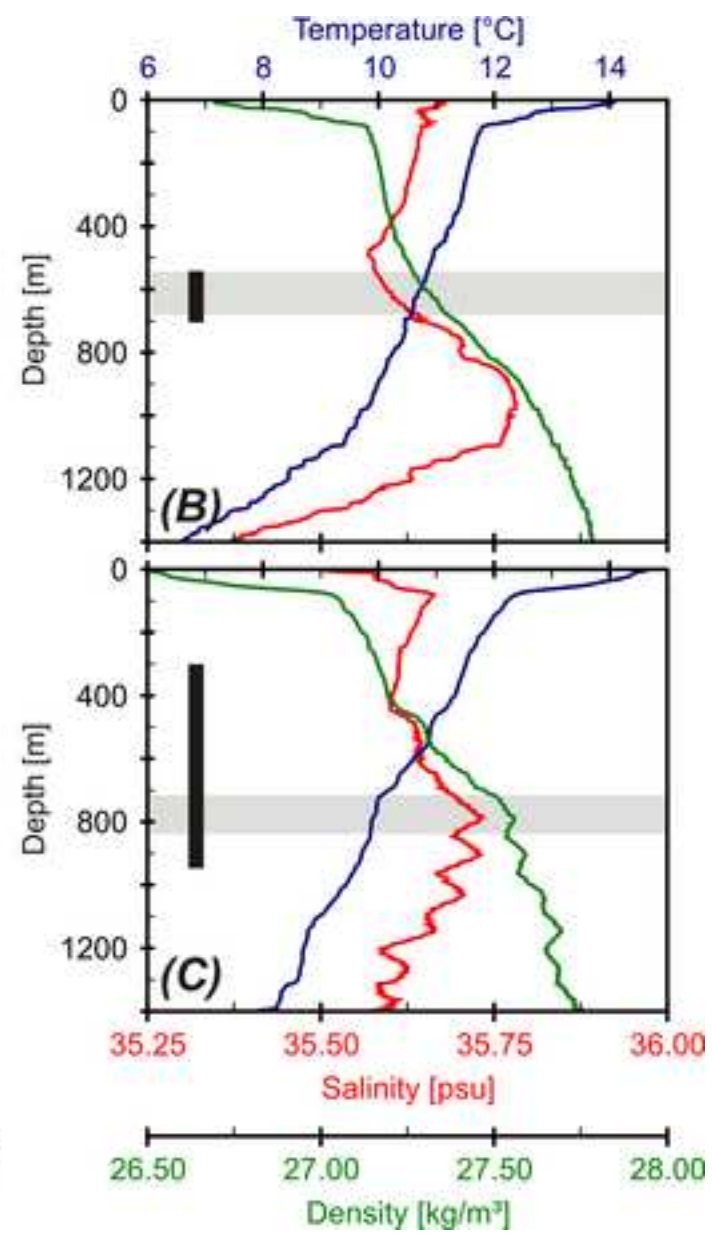
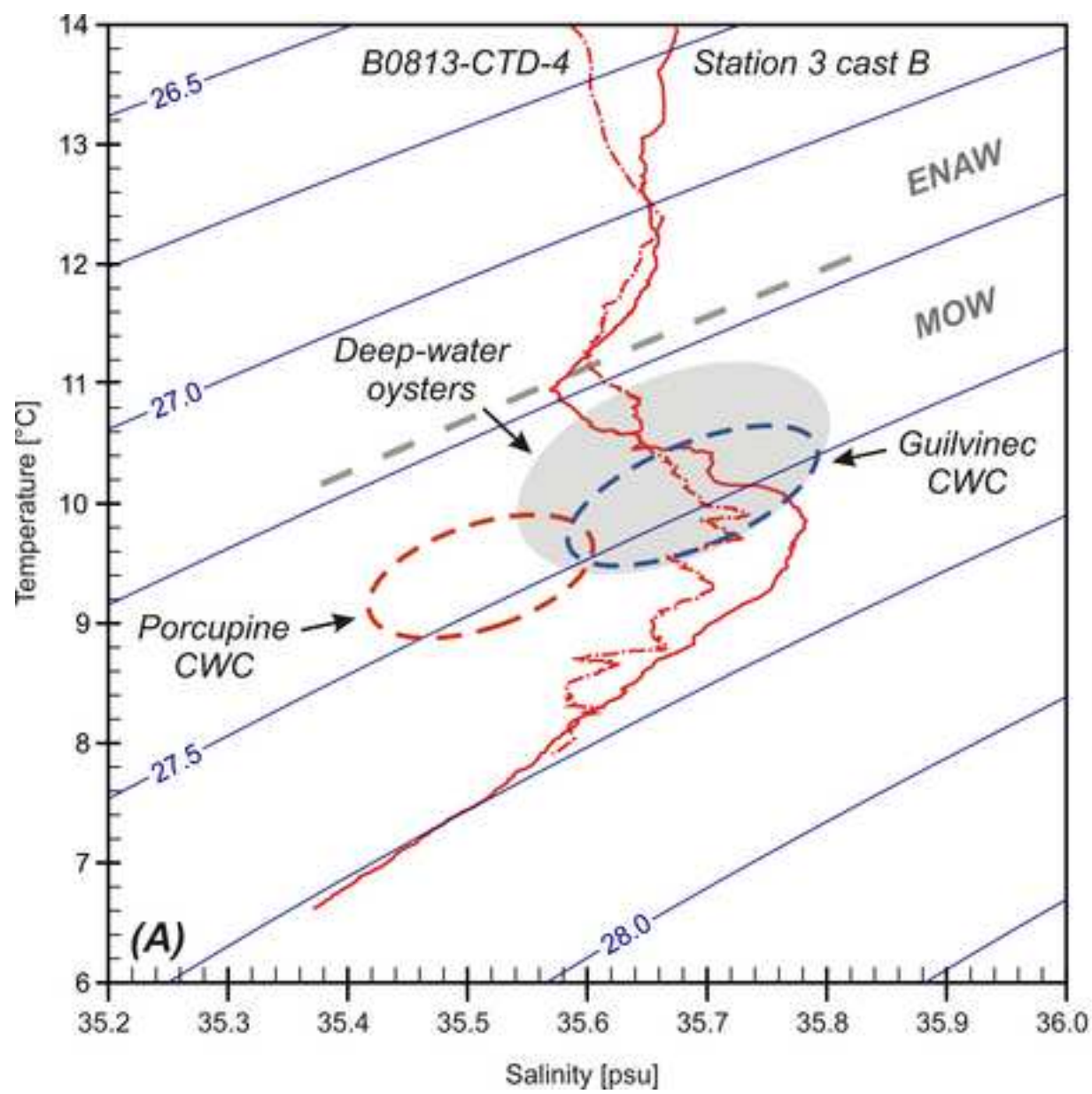


Figure 03
[Click here to download high resolution image](#)

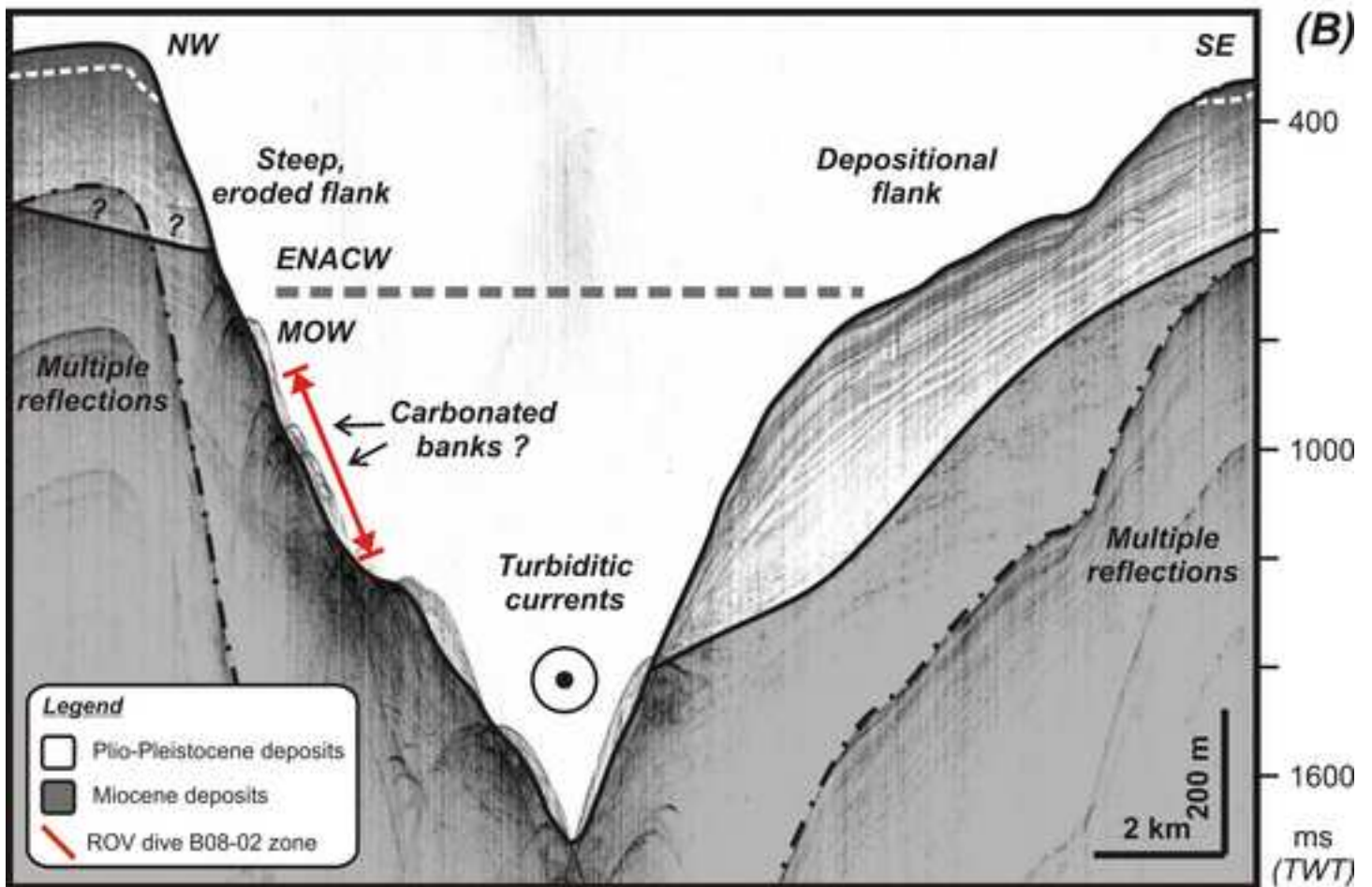
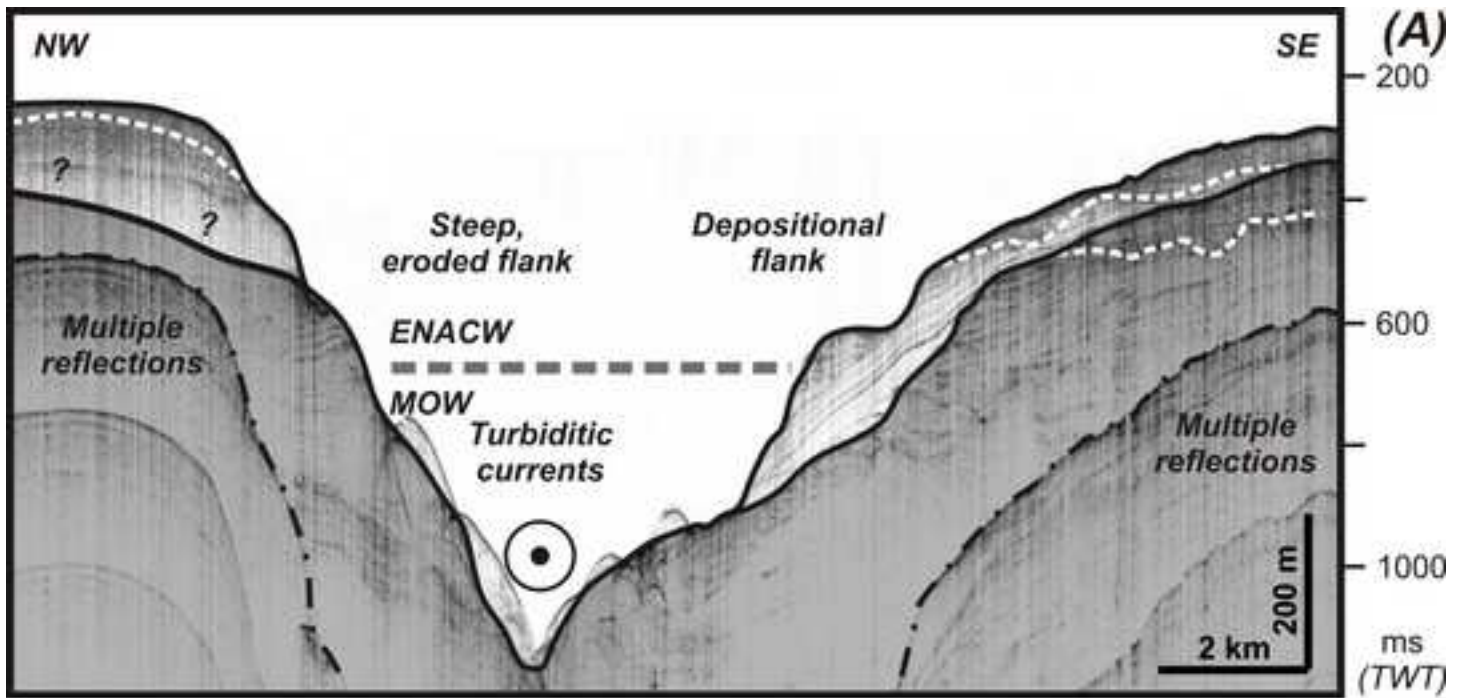


Figure 04
[Click here to download high resolution image](#)

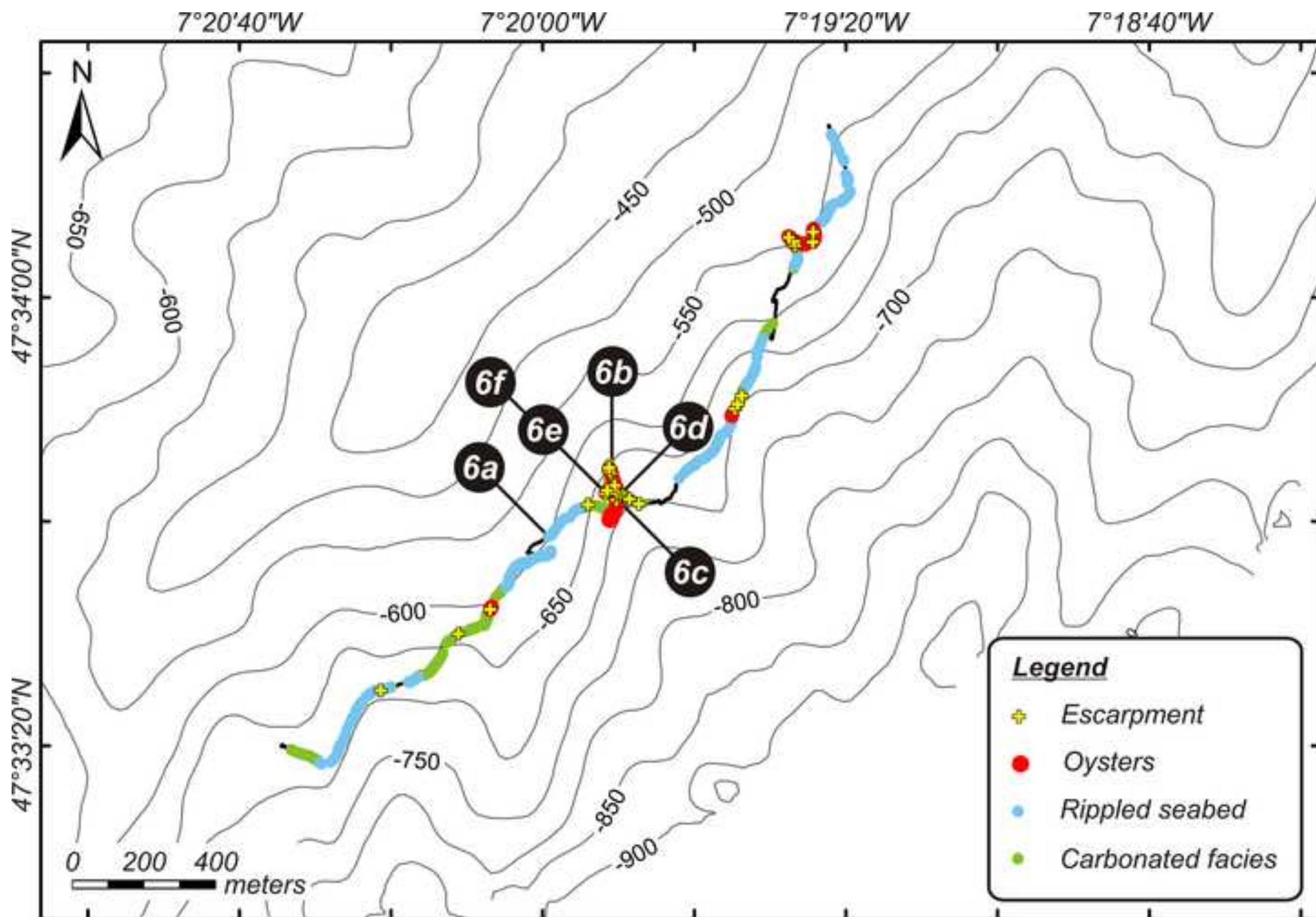


Figure 05

[Click here to download high resolution image](#)

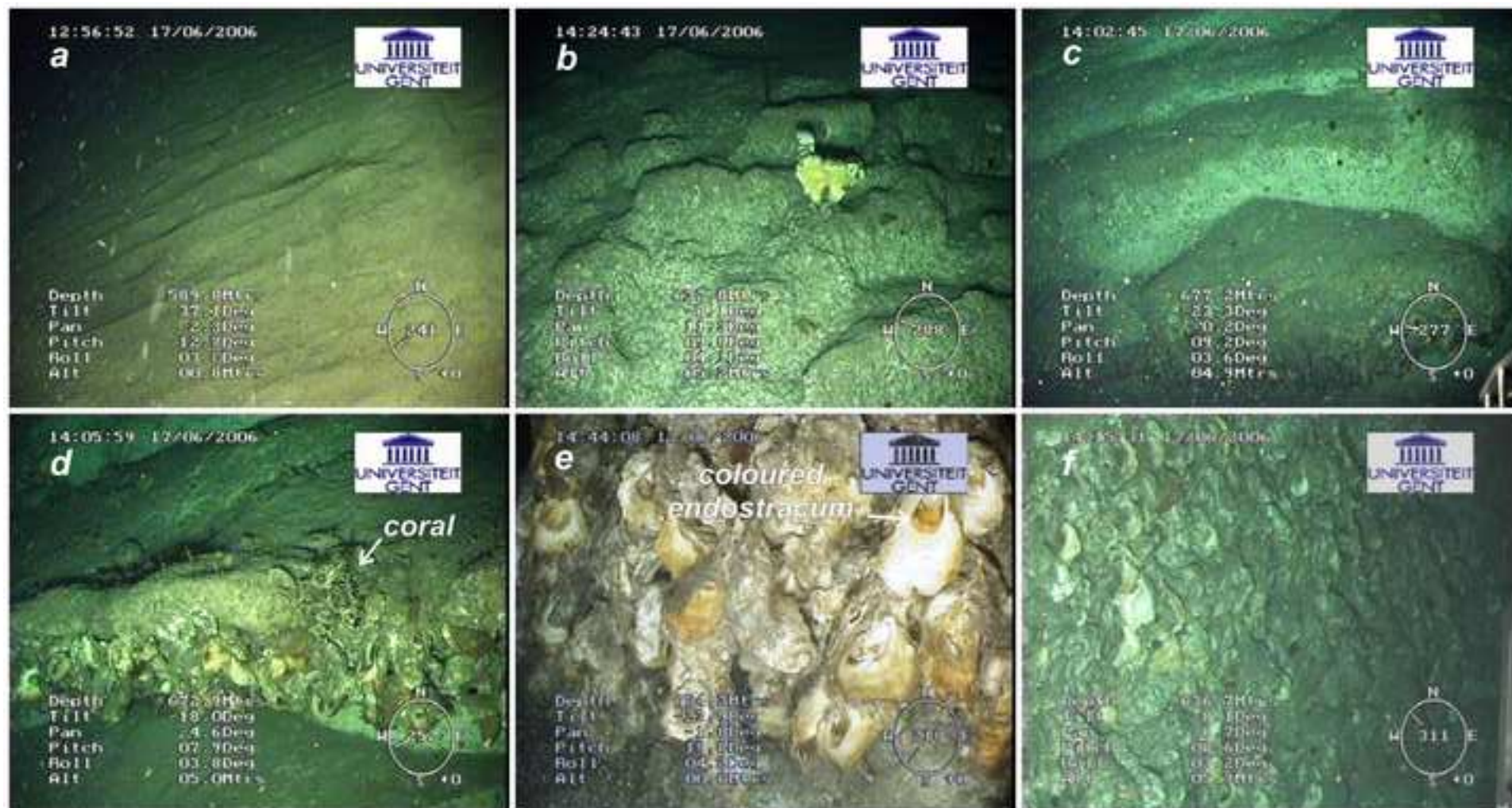


Figure 06
[Click here to download high resolution image](#)

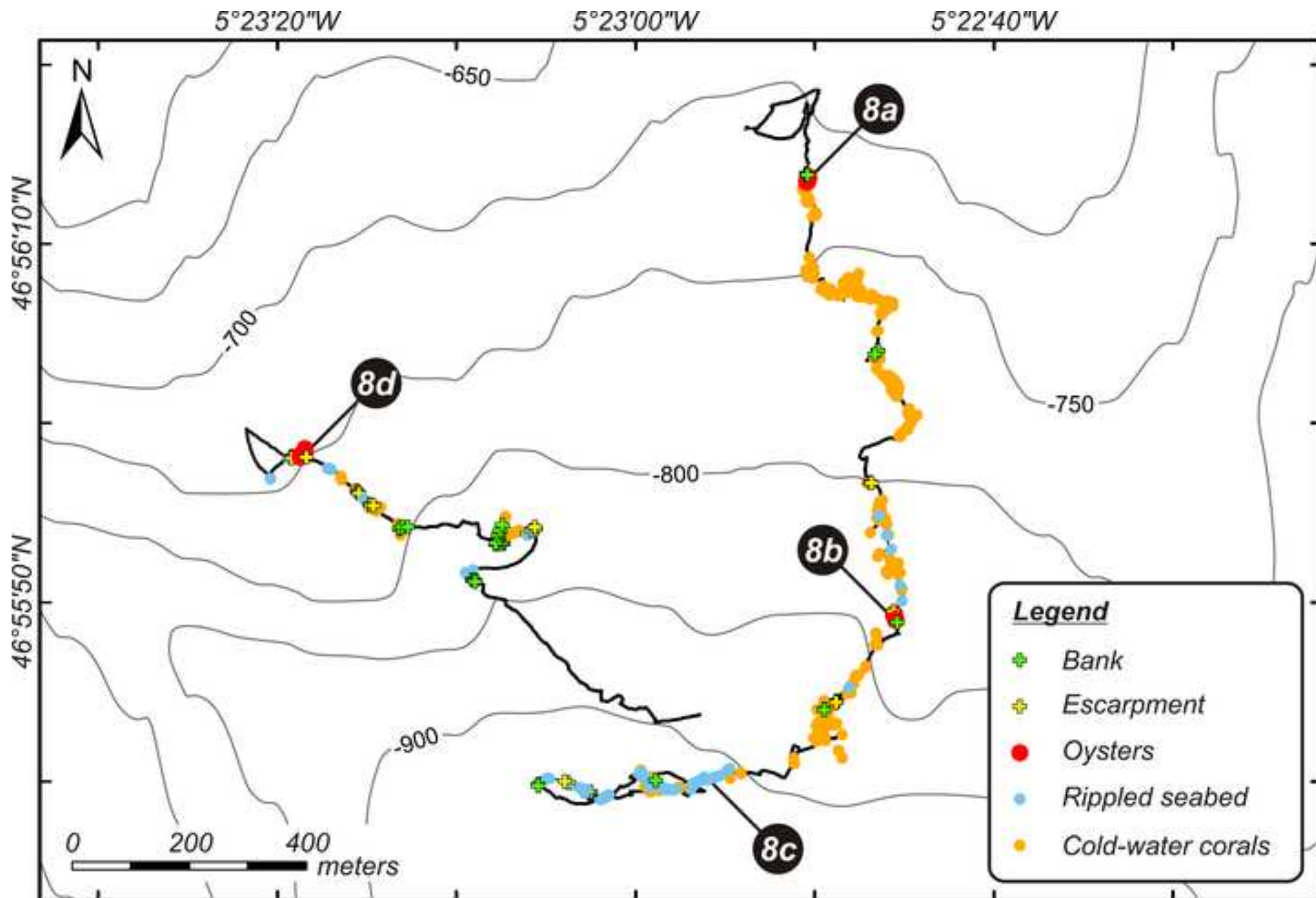


Figure 07
[Click here to download high resolution image](#)

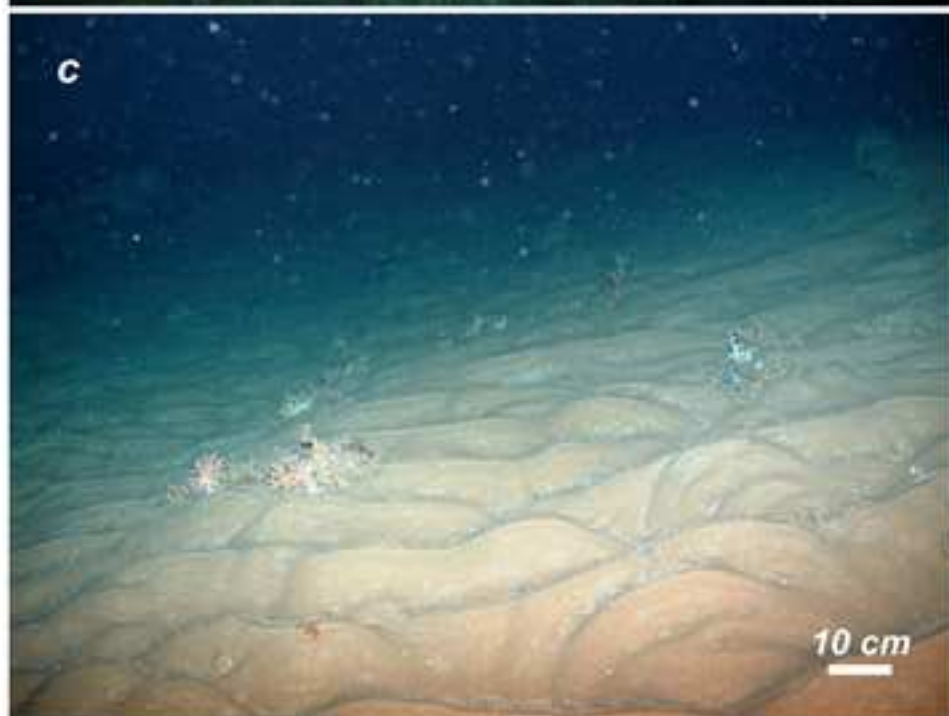
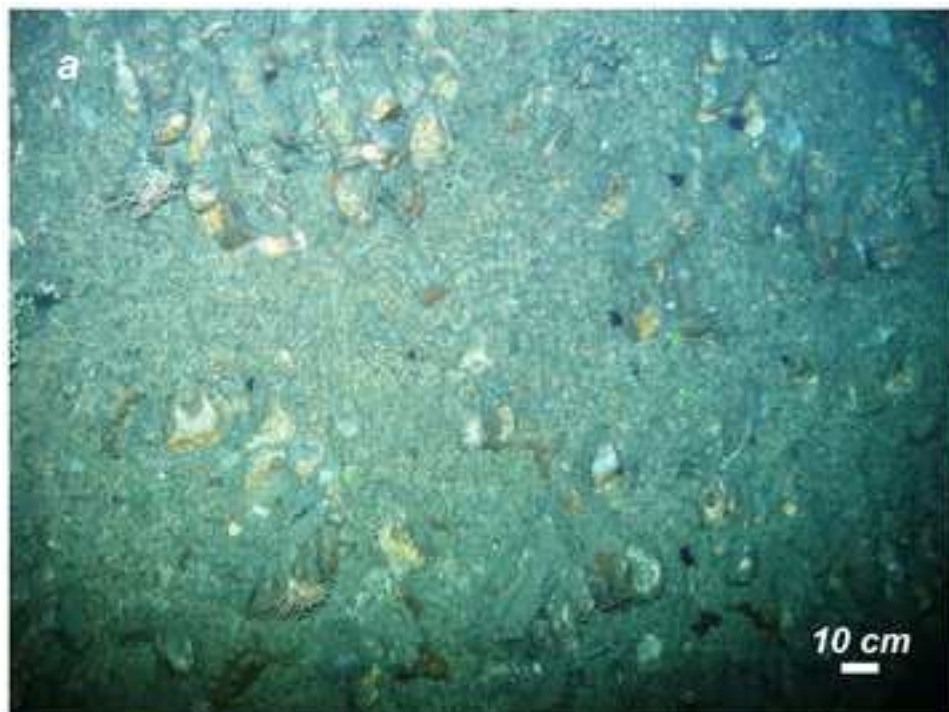


Figure 08
[Click here to download high resolution image](#)

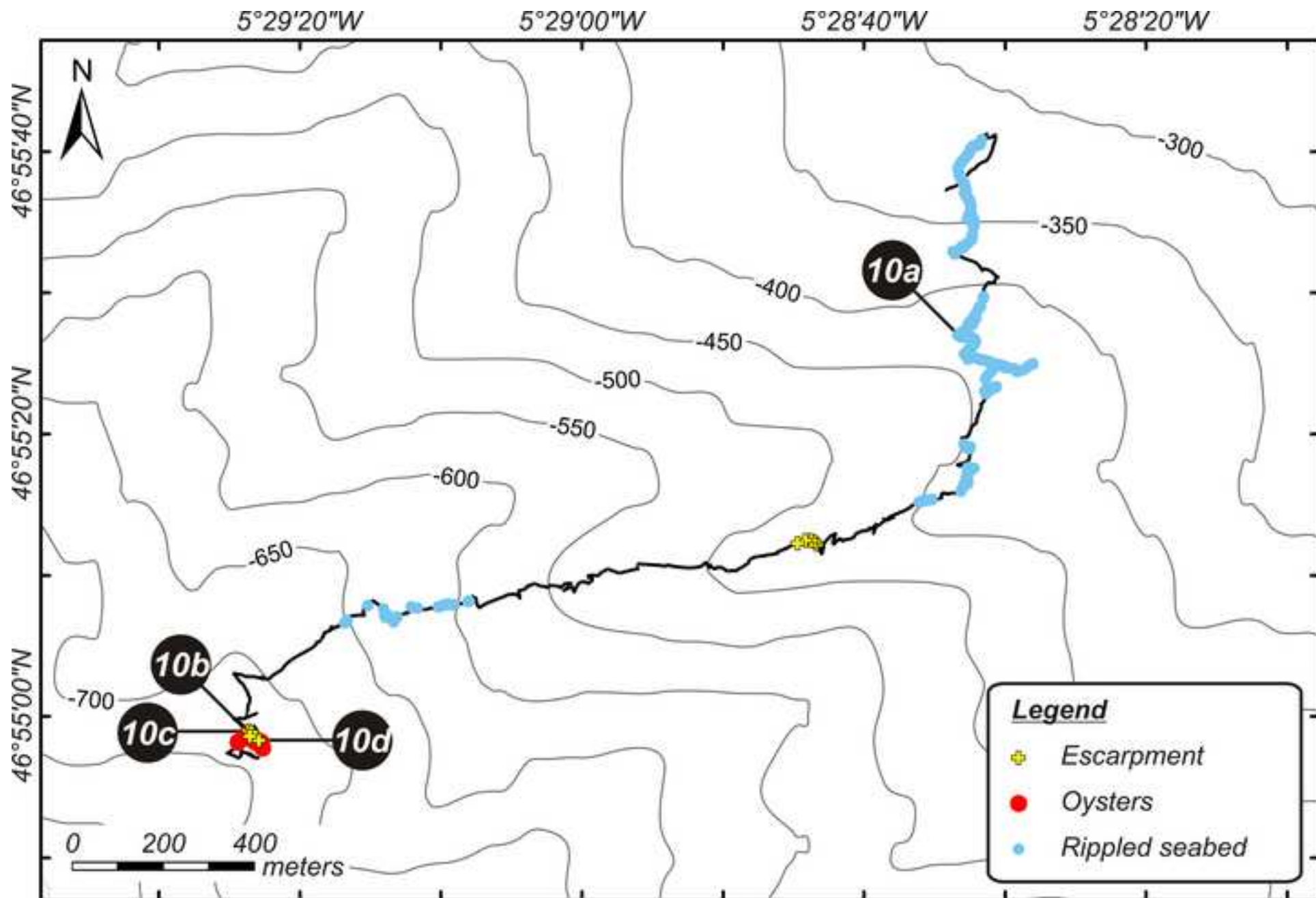


Figure 09
[Click here to download high resolution image](#)

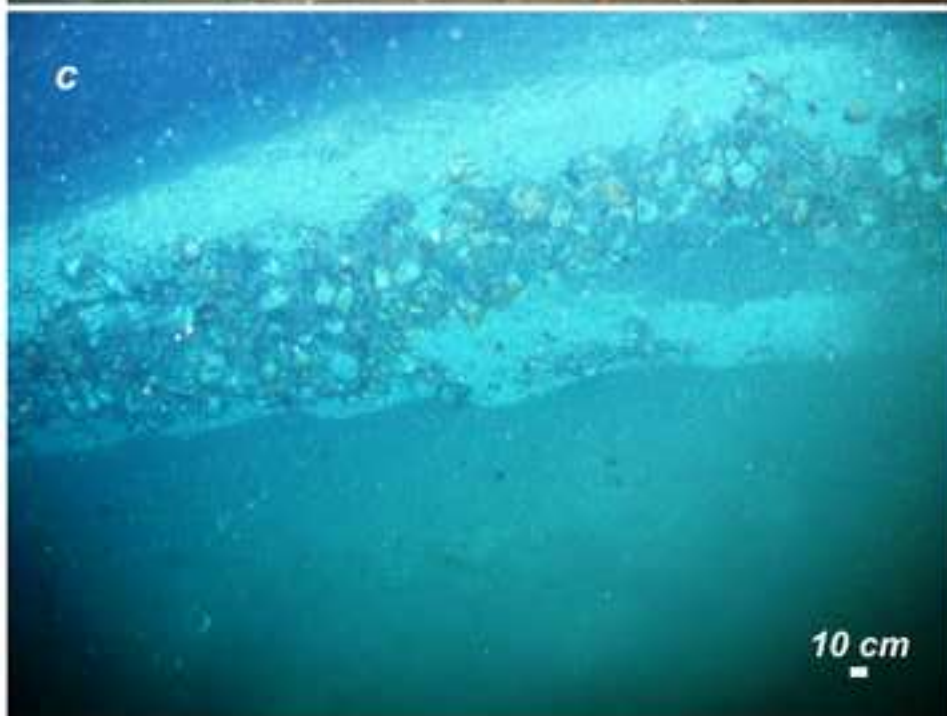
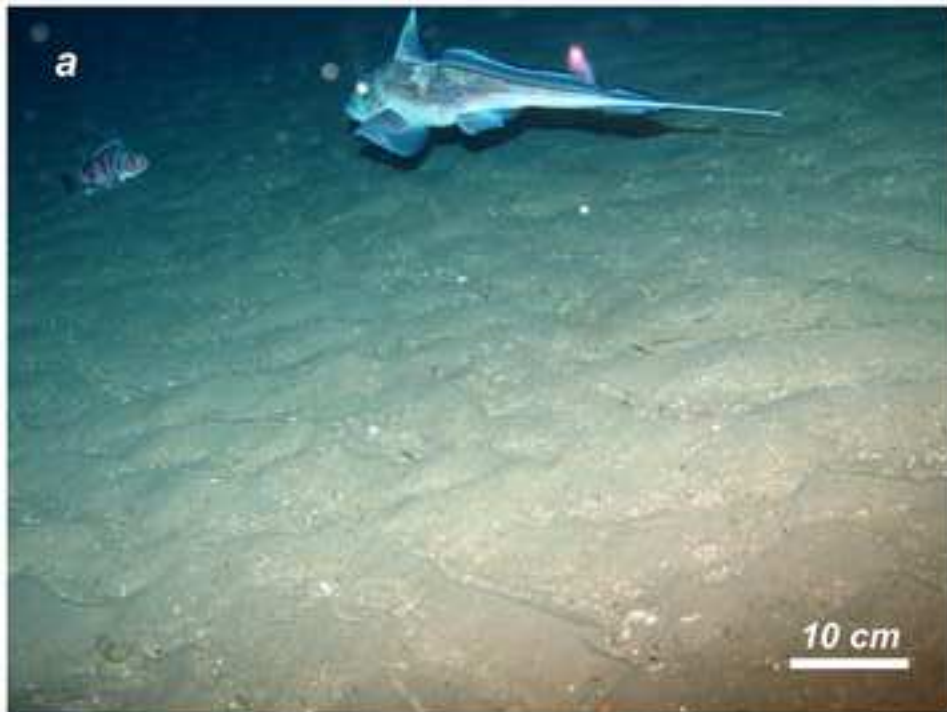


Figure 10
[Click here to download high resolution image](#)

